Study on Preparation and Photocatalytic Activity of Carbon Modified N-TiO_2/montmorillonite Composite

2018, March

Jiannan Hsing

Graduate School of Environmental and Life Science

(Doctor's Course)

OKAYAMA UNIVERSITY

Abstract

TiO_2/clay composites are materials prepared by intercalation of TiO_2 particles into the aluminosilicate interlayers of clay materials. Due to the special properties of TiO_2/clay composites, TiO_2/clay composites were suggested as one of the most competitive candidate for applications to photocatalytic decomposition of organic contaminants in water. The morphological structure of TiO_2/clay composites results in a huge amount of micropores and mesopores which can greatly enhance the adsorption capacity of organic contaminants. Compared with bare TiO_2 photocatalyst, the photocatalytic activities of TiO_2/clay composites are improved by the enrichment of organic contaminants caused by the enhanced adsorption capacity. In spite of such advantage in photocatalysis, TiO_2/clay composites has the same problem as well as TiO_2 photocatalyst. TiO_2 is a wide bandgap semiconductor(e.g., anatase, 3.2 eV). The wide bandgap supplies very strong oxidizability on photocatalytic decomposition of organic materials, on the other hand, requires very high photon energy so that photoexcitation of electrons and positive holes can be generated. Thereby, the powerful photocatalytic activity of TiO_2 are presented only under UV light irradiation which constitutes about 4% of solar light.

To achieve high performance TiO_2/clay composite, the first concerned problem that limits photocatalytic activity should be the narrow responsive light region of TiO_2. In this thesis, our attempt is to enhance the photocatalytic activity of TiO_2/clay composite under visible light irradiation. Two modification methods, nitrogen doping and carbon deposition were both employed for improving the photocatalytic activity.

Nitrogen doping is an effective method to enhance photocatalytic activity by modification of the TiO_2 bandgap. The nitrogen inions introduced by nitrogen doping arise two different chemical states, either substitutional N or interstitial N. In both cases, an isolated N 2p midgap is generated above the top of the valence band, reducing the bandgap energy of TiO_2. Thus, photoexcitation of electrons is available under visible light irradiation which contains relatively lower photon energy. However, nitrogen doping induces oxygen vacancies act as recombination centers of photoexcited electrons and positive holes, decreasing the lifetime of photoexcited electrons and positive holes. Therefore, how to effectively facilitate the separation of photoexcited

electrons and positive holes is one of the determinant factors to improve photocatalytic activity.

Carbonaceous materials have excellent chemical and electrical properties. The utilization of carbonaceous nanomaterials to improve the photocatalytic activity of TiO_2 has attracted increasing attention. It is reported that the carbon modified TiO_2 exhibits enhanced photocatalytic activity due to effective retardation to the recombination of photoexcited electrons and positive holes. Some research have revealed that the photocatalytic activity could be enhanced by carbonaceous species after incomplete calcination procedures. It may be suggested a new modification method for TiO_2 catalyst, effective and easy to operate under lower calcination temperature.

This thesis is constructed with four chapters and summarized below:

In Chapter 1, the background of organic water pollution and the overview of TiO_2 catalyst and TiO_2/clay composite was carefully introduced. Meanwhile, the object of this thesis, to develop high active visible light responsive TiO_2/clay composite, has been proposed, accordingly.

In Chapter 2, the nitrogen doped TiO_2/montmorillonite(NTM) composite was prepared via sol-gel method, in which urea(as nitrogen source) is introduced into TiO_2 precursor. Two points, 1) The effect of N / Ti ratio on photocatalytic activity and 2) the effect of calcination temperature on photocatalytic activity were mainly discussed, via characterization and evaluation of photocatalytic activity.

According to the characterization results, the phase of the intercalated TiO_2 particles in both cases of NTM samples(the sample with various N / Ti ratio and the samples with various calcination temperature) were identified as anatase. With increasing the N / Ti ratio of the NTM composite, the absorbance around 400 to 600 nm enhanced gradually due to the fact that nitrogen cations introduced in TiO_2 crystalline act as chromophoric centers. When raise the calcination temperature, the absorbance enhanced gradually, but stop to decrease over 350°C. The decreased absorbance was attributed to the fact that calcination may lead to nitrogen loss at high temperature. The decomposition of Bisphenol a (BPA) was carried out for evaluation of photocatalytic activity. From the results, it is worth to notice that the decomposition of BPA in the absence of irradiation or without a photocatalyst was almost negligible. Consequently, the adsorption

behavior of BPA is almost negligible while the discussion on photodecomposition of BPA becomes much important. When the N / Ti ratio of the NTM composite was increased, the decomposition rate of BPA increased until the N / Ti ratio up to 1.5, and then became to decrease gradually due to the fact that high doping amount leads to a large number of oxygen vacancies. These defects of crystalline in TiO_2 may act as recombination centers of photoexcited electrons and positive holes, greatly decreasing the photocatalytic activity. The optimum calcination temperature was 250°C. With further raising the calcination temperature, the photocatalytic activity decreased. The decrease of photocatalytic activity was attributed to decreased basal spacing of montmorillonite caused by dehydration of TiO_2 particles, and thus suppressed the photocatalytic activity.

In Chapter 3, the carbon deposited N-doped TiO_2/montmorillonite(CNTM) composite was prepared with carbon modification. Ethanol, as the carbon source, was added into the N-doped TiO_2/montmorillonite colloidal, treating with low temperature calcination. Characterization and evaluation photocatalytic activity were carried out in order to understand 1) the differences between the NTM composite and CNTM composite, 2) the effect of carbon content on photocatalytic activity.

According to the characterization results, the carbon modification have made great effect on the properties of the CNTM composite but no observable effect on crystalline structure was found. An obviously color change over visible light region was attributed to carbon modification. The absorbance of the CNTM composite depended on carbon content which increased with increasing ethanol dosage. Due to no observable carbon phase was observed, the carbonaceous species introduced into the CNTM composite are supposed to be amorphous carbon. These carbonaceous species was probably generated at nano-size and deposited on the TiO_2 particles. The carbon modification resulted in remarkable enhancement of photocatalytic activity on decomposition of BPA under visible light irradiation and negligible effect on adsorption of BPA. The high photocatalytic activity of the CNTM composite was due to the co-catalysis of nitrogen doping and carbon deposition. Firstly, nitrogen doping enabled visible light response of TiO_2 particles in the composite, leading to photoexcitation of electrons and positive holes under visible light irradiation. Meanwhile carbonaceous species act as charge accepters so that the electrons or holes can transfer from the TiO_2 particles to the carbonaceous species freely, thus suppressed the recombination of photoexcited

electrons and positive holes. Consequently, the longtime lived electrons and positive holes had increased chance to react with the adsorbates in photocatalysis reaction. Furthermore, the effect of carbon content on photocatalytic activity was discussed. The results shows that the carbon content depended on ethanol dosage and make obviously effect on photocatalytic activity. The optimum ethanol dosage to prepare the CNTM composite was 2 mL/g. Heavy ethanol dosage resulted in excessive amount of carbonaceous species, which may cause interference to TiO_2 particles from absorbing visible light.

In Chapter 4, the summary of this thesis was provided and the prospects of this research was placed.

Contents

Chapter 1 Introduction

1.1 Background

Water pollution is one of the global crises, which has posed a greater threat to the natural environment and human health in both developing and industrialized nations. Public health and environmental concerns have driven great effort to raise awareness of this global crisis. However, the quantity of wastewater discharge cannot be effectively controlled due to the growth of world population and irregular world industry. Apparently, the threat from water pollution will continue in the coming decades[1]. The hazardous pollutants in wastewater include: solvents, surfactants, dyes, pharmaceuticals, pesticides, endocrine disrupters, dioxins, asbestos, heavy metals and arsenic compounds etc.[2-9] Most of them are organic compounds, which are high-toxic substances or complete carcinogen in addition to very hard to naturally degrade via environmental self-purification[10-16]. Hazardous organic pollutants have been detected from both underground water, surface waters, sea waters, and even drinking waters[17-23], due to traditional biological treatment is inadequate to completely decompose and remove refractory organics in water. Therefore, human health and ecological system are taking serious threat[24-26] as if the hazardous organic pollutants cannot be removed completely from wastewater. Extensive research is underway to seek an advanced water treatment method, which should be effective, easy-to-operate and low-cost in-situ methods for water purification, without secondary pollution or endangering ecological system and human health by the treatment itself[27-30].

1.2 TiO_2 photocatalyst

Advanced physicochemical method such as semiconductor photocatalysis is intended to be supplementary and complementary to traditional treatment for elimination of hazardous organic pollutants in water. Utilization of inexhaustibly abundant and clean solar light is expected to be a major advance in the development of sustainable, non-

hazardous, and lower-cost water treatment method[31]. A typical semiconductor photocatalyst, titanium dioxide, also known as titania or TiO_2 is suggested to be the appropriate photocatalyst. Since photocatalytic water splitting with TiO_2 was discovered in 1972 by Fujishima and Honda[32], TiO_2 has attracted considerable academic attentions as photocatalyst due to its high photoctalytic activity in the non-selective decomposition of organic pollutants[33]. In addition, TiO_2 has also exhibited its unique advantages on water splitting[34-36], solar cells[37,38], antibacterial[39], and inhibition of cancer[40].

1.2.1 TiO_2 photocatalyst and its elementary mechanism

Under certain light irradiation, the organic pollutants adsorbed on the surface of TiO_2 or within the surrounding charged particles can be decomposed via vigorous oxidation. The elementary mechanism has been generally described while a number of processes, which have been discussed exhaustively in the literatures[41,42]. It is commonly agreed that the primary photocatalytic transformation is interfacial redox reactions of electrons and holes (Figure 1.1). The electronic structure of TiO_2 is characterized by a filled valence band and empty conduction band[43]. When a photon with abundant energy of hν (no less than the band gap energy, E_g), an electron from the valence band is excited, then jump into the conduction band, leaving a hole behind.

$TiO_2 + h\nu \rightarrow h^+ + e^-$

The recombination of excited conduction-band electrons and valence-band holes occurs concomitantly in the absence of suitable electron and hole scavengers. Most of the electrons and holes recombine within a few nanoseconds, resulting in quantum emission of energy as fluorescence or dissipate the input energy as heat.

$h^+ + e^- \rightarrow$ heat

Remaining electron-hole pairs diffuse to the surface of TiO_2 particles, leading to the interface charge transfer. Some of the electron-hole pairs get trapped in metastable surface states. The photoexcited electrons can reduce the surface titanium atom from Ti(IV) to yield Ti(III) while the Ti(III) atom is re-oxidized by the next available hole

(essentially the same as recombination).

$Ti^{+4} + e^{-} \rightarrow Ti^{+3}$

$Ti^{+3} + h^{+} \rightarrow Ti^{+4}$

The rest electron-hole pairs react with electron donors and acceptors adsorbed on the TiO_2 surface. In particular, an organic compound is oxidized by the holes which are powerful oxidants.

$h^{+} + RH \rightarrow R^{\bullet} + H^{+}$

Hydroxyl radicals are formed on the surface of TiO_2 by the reaction of holes with adsorbed water or hydroxide.

$h^{+} + H_2O \rightarrow OH^{\bullet} + H^{+}$

$h^{+} + OH^{-} \rightarrow OH^{\bullet}$

Meanwhile, the photoexcited electrons reduce oxygen and form superoxide radical anion, which is an intermediate in the production of hydrogen peroxide.

$e^{-} + O_2 \rightarrow O_2^{\bullet -}$

$O_2^{\bullet -} + H^{+} \rightarrow HO_2^{\bullet}$

$e^{-} + HO_2^{\bullet} + H^{+} \rightarrow H_2O_2$

$2HO_2^{\bullet} \rightarrow H_2O_2 + O_2$

Hydroxyl radicals are produced from the decomposition of hydrogen peroxide.

$H_2O_2 + O_2^{\bullet -} \rightarrow OH^{\bullet} + OH^{-} + O_2$

$H_2O_2 + e^{-} \rightarrow OH^{\bullet} + OH^{-}$

The organic pollutants present in aqueous or gas phase can be easily attacked by hydroxyl radicals, which is highly reactive, play an important role in the oxidative decomposition by using a series of methodologies collectively known as advanced oxidation processes (AOPs)*[44,45]*.

$OH^{\bullet} + RH \rightarrow R^{\bullet} + H_2O$

Due to the lack of a hydrogen atom, the resulting alkyl radical will typically react rapidly with oxygen, leading organic pollutants to CO_2 and water, the final products of mineralization. The vast majority of organic pollutants can be decomposed either directly or indirectly or both in the photodecomposition reaction.

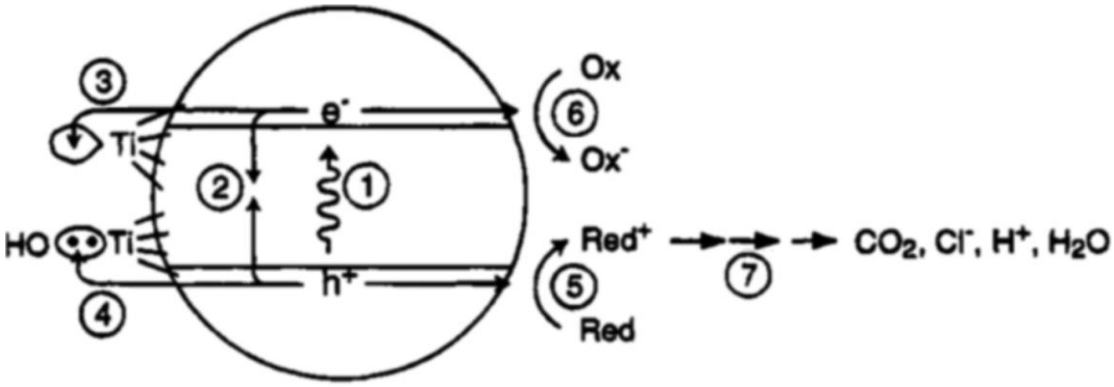

Fig. 1.1 Primary processes in the mechanism of photocatalysis: (1) generation of excited electrons and holes by photon absorption; (2) recombination of excited electrons and holes; (3) trapping of a conduction-band electron at a Ti(IV) site to yield Ti(III); (4) trapping of a valence-band hole at a surface excited electrons and holes group; (5) initiation of an oxidative pathway by a valence-band hole; (6) initiation of a reductive pathway by a conduction-band electron; and (7) further thermal (e.g., hydrolysis or reactions with active oxygen species) and photocatalytic reactions to yield mineralization products. (adapted from *Ref. 31*)

1.2.2 Visible light responsive TiO_2 photocatalyst

TiO_2 has been proven to be a great potential photocatalyst, however, the photodecomposition of organic pollutant by TiO_2 are only effective under UV light irradiation. Despite UV light exists in solar light, the 4% of solar light is inadequate for TiO_2 to present its full performance. In order to efficiently use light energy, thus scale up the applications of TiO_2, attempts have been launched for years to extend the light responsive edge of TiO_2 from UV light into visible light range. As shown in the mechanisms of TiO_2 photocatalysis, the amount of photoexcited electrons and holes participating in the photoredox reaction makes a great effect on improving the photocatalytic activity of TiO_2. How to produce available photoexcited electrons and holes under visible light irradiation is one key point in visible light response of TiO_2. Therefore, modification of the band gap of TiO_2 is expected to be effective to increase the amount of photoexcited electrons and holes under visible light irradiation.

A variety of modification methods have been approached, such as chemical doping*[46-48]*, semiconductor coupling*[49]*, dye sensitization*[50]*, etc. The modification of TiO_2 via chemical doping have shown comparatively excellent effects on the enhancement of photocatalytic activity under visible light irradiation. In general, chemical doping of TiO_2 is divided into metal doping and nonmetal doping. In the metal doping method, a

certain amount of metal (mainly 3d-transtion metals, such as Fe, Cr, Ru, Ce, La, and V) ions are introduced into the crystal lattice of TiO_2[51-56], creating an impurity state between the minimum of the conduction band and the maximum of the valence band. The impurity states introduced by metal doping can successfully extend the absorption edge of TiO_2 from UV light to the visible light range, thus effectively improve the photocatalytic activity of TiO_2 under visible light irradiation. On the other hand, the introduced impurity state also leads to thermal instability of the doped TiO_2[57] and increasd recombination centers of photoexcited electron and holes[58].

Another doping method, nonmetal doping is achieved by substitution of lattice oxygen with nonmetal elements, such as B, C, N, F and S of which atomic radius is similar to that of the O atom. Unlike metal doping method, the modified TiO_2 via nonmetal doping shows better thermal stability and synthetically lower cost. In 2001, Asahi et al.[47] reported that nitrogen-doped TiO_2 (N-TiO_2) exhibits an obvious visible light absorption and enhanced photocatalytic activity under visible light irradiation. They also calculated densities of states (DOS) of the nonmetal-doped anatase which is modified by employing C, N, F, P, and S as dopants demonstrated that nitrogen was the most promising element for nonmetal doping. Since then, researches concerning nonmetal-doped TiO_2, in particular N-TiO_2, has become quite a popular direction. Nevertheless, the origin of visible light responsive property of TiO_2 is still under debate, in particular the photocatalytic mechanism of nitrogen doping[58,59]. Recent experimental and theoretical studies reach a relatively concordant agreement that the nitrogen anion introduced by nitrogen doping arise an isolated midgap above the maximum of the valence band of TiO_2 rather than narrowing the bandgap of TiO_2, reducing the band gap energy of TiO_2[58,60-64]. Thereby, photoexcited electrons and holes can be generated under visible light irradiation. Although the mechanism of nitrogen doping for TiO_2 seems to be not theoretically clear, the applications of N-TiO_2 have begun since the 2000s. By now, it is known that N-TiO_2 has been used in textile, upholstery, tooth bleaching, air and water purification systems.

1.3 TiO_2/clay composites

1.3.1 Montmorillonite

Montmorillonite is world-wide applied as a host material for synthesis of a variety of intercalation compounds and composites[65,66]. The structure of montmorillonite[67-69] is shown in Fig. 1. 3. Isomorphic substitutions of Si^{4+} by Al^{3+} in the tetrahedral layer and/or of Al^{3+} by Mg^{2+} in the octahedral layer results in negative charge of the layers of montmorillonite. The exchangeable cations, such as Na^{+}, Ca^{2+} exist between the unit layers (or in the interlayer space) as surface complexes for keeping the charge balance. Therefore, montmorillonite exhibits cation remarkable cation exchange capacity in addition to a relatively higher adsorption capacity.

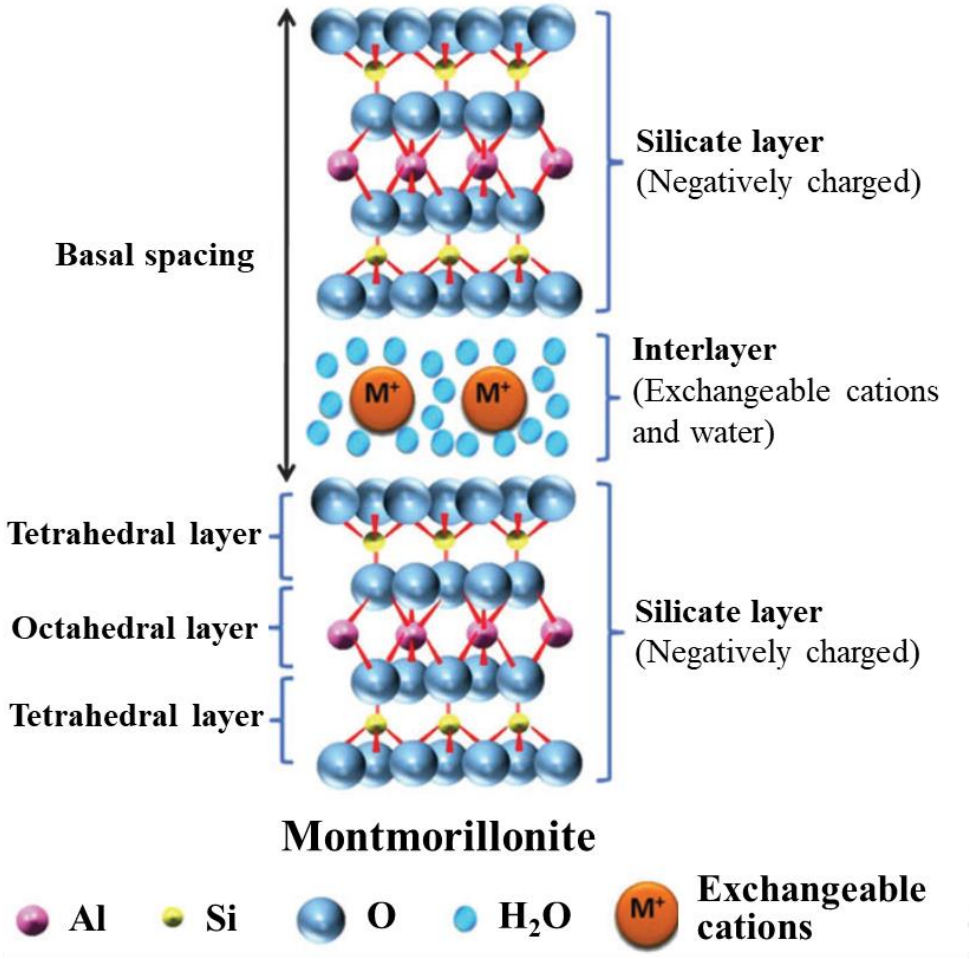

Fig. 1.3 Structure of montmorillonite

1.3.2 Pillared clay

TiO_2/clay composites are pillared clays, which are intercalated by TiO_2 particles between aluminosilicate layers of clay materials. TiO_2/clay composites are suggested as one of the suitable materials for the applications on environmental decontamination, such as photodecomposition of organic contaminants[70-72]. The porous structure of TiO_2/clay composites provides large specific surface area, leading to strong adsorption of organic contaminants. Compared with a bare TiO_2 photocatalyst, TiO_2/clay composites exhibit higher photocatalytic activity due to the fact that the enrichment of organic contaminants increases the possibility of molecular encounter which plays an important role in chemical reaction[73,74]. Another advantage of TiO_2/clay composites is easier separation from water. As we known, most of TiO_2 photocatalysts are prepared into nanosized particles in order to improve photocatalytic activity. However, nanosized TiO_2 lead to a super hydrophilic phenomenon[75] on the surface of the particles, especially for anatase which is the most used phase of TiO_2 for photodecomposition. It is certain that the bared TiO_2 photocatalysts requires an additional and somewhat complex operation to separate it out from the solution after photodecomposition. By contrast, application of TiO_2/clay composites can well resolve this practical problem due to the hydrophobic silicate layers of clay. In addition, clay materials are harmless material to the environment and human health. The TiO_2/clay composite will not result in secondary pollution or endangering ecological system and human health. Research on the TiO_2/clay composite is of great interest, meanwhile offer opportunities for the design of new photocatalytic systems.

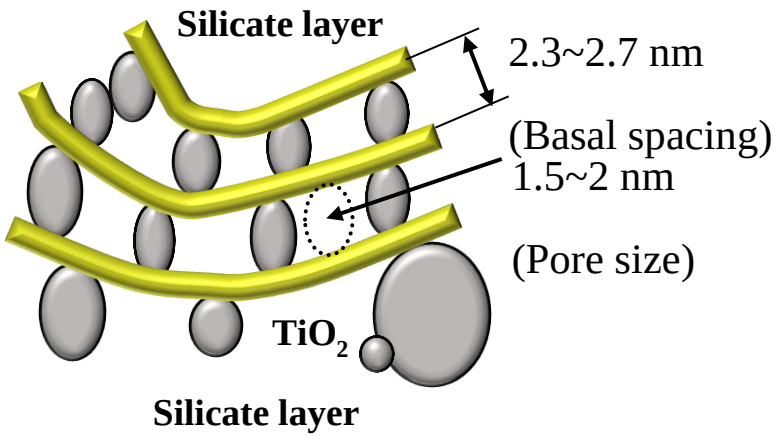

Figure 1.3. Scheme of TiO_2/clay composite.

In recent years, investigations concerning TiO_2/clay composites with the visible light response have been reported. G. K. Zhang et al*[76]*., synthesized N, S-codoped TiO_2 pillared montmorillonite which has promoted photocatalytic activity for the decomposition of 4BS dye under visible light irradiation. Another approach, V-TiO_2/montmorillonite nanocomposites with visible response were successfully prepared by sol-gel method*[77]*. Sasai et al.*[78]*, reported a kind of dye sensitized organo-pillared clays, with cationic Cu-phthalocyanine derivatives as photosensitizers, exhibited a remarkable adsorption capacity and effective photocatalytic activity to bisphenol A under visible-light irradiation. J. Zhang et al.*[79]*, reported that a novel and efficient attapulgite composite with the visible light response was prepared by introducing BiOBr-TiO_2 hybrid oxides onto its surface by using in-situ deposition. Despite a variety of attempts to promote the photocatalytic activities of TiO_2/clay composites under visible light irradiation, many principle roles, e.g., the effect of the clay materials in electron transportation when electrons and holes generated, are still far from being understood today. Besides, there is also a great potential for further exploitation of new TiO_2/clay composites which are effective, low-cost and easy to synthesize.

1.4 Objective of this thesis

TiO_2/clay composite was suggested as one of the most competitive candidates for applications to photocatalytic decomposition of organic contaminants in water. However, TiO_2/clay composite has the same problem as well as TiO_2 photocatalyst. Due to the fact that the powerful photocatalytic activity of TiO_2 is presented only under UV light irradiation, the photocatalytic activity of TiO_2/clay is under limit. To achieve high performance TiO_2/clay composite, the first concerned problem that limits photocatalytic activity should be the narrow responsive light region of TiO_2. In this thesis, our attempt is to enhance the photocatalytic activity of TiO_2/clay composite under visible light irradiation. Two modification methods, nitrogen doping and carbon deposition were both employed to improve the photocatalytic activity. Nitrogen doping was employed in preparation of N-TiO_2/montmorillonite composite, which is expected to extend the absorption range into visible light and enhanced photocatalytic activity. Then, a following approach in order to further improve the photocatalytic activity of N-TiO_2/montmorillonite composite have been proposed. Carbon deposition was employed for modification of N-TiO_2/montmorillonite composite. A novel photocatalyst, carbon deposited N-TiO_2/montmorillonite composite was expected to achieve.

1.5 Reference

1. M. A. Shannon, Science and technology for water purification in the coming decades, nature. 452 (2008) 301–310.
2. Y. Ohko, I.Ando, C. Niwa, T. Tatsuma, T. Yamamura, T. Nakashima, Y. Kubota, A. Fujishima, Degradation of bisphenol A in water by TiO_2 photocatalyst. Environ. Sci. Technol. 35 (2001) 2365–2368.
3. T. Yamamoto, A.Yasuhara, H. Shiraishi, O. Nakasugi, Bisphenol A in hazardous waste landfill leachates. Chemosphere. 42 (2001) 415–418.
4. M. Pera-Titus, V. García-Molina, M.A. Baños, J. Giménez, S. Esplugas, Degradation of chlorophenols by means of advanced oxidation processes: A general review, Appl. Catal. B: Environ. 47 (2004) 219–256.
5. A. Pal, K.Y.-H. Gin, A.Y.-C. Lin, M. Reinhard, Impacts of emerging organic contaminants on freshwater resources: Review of recent occurrences, sources, fate and effects, Sci. Total Environ. 408 (2010) 6062–6069.
6. C. S. Guo, Directed Synthesis of Mesoporous TiO_2 Microspheres: catalysts and their photocatalysis for bisphenol A degradation, Environ. Sci. Technol. 44 (2010) 419–425.
7. J.O. Tijani, O.O. Fatoba, G. Madzivire, L.F. Petrik, A review of combined advanced oxidation technologies for the removal of organic pollutants from water, Water Air Soil Pollut. 225 (2014) 2102.
8. M. Capocelli, E. Joyce, A. Lancia, T.J. Mason, D. Musmarra, M. Prisciandaro, Sonochemical degradation of estradiols: Incidence of ultrasonic frequency, Chem. Eng. J. 210 (2012) 9–17.
9. B. Jiang, J. Zheng, S. Qiu, M. Wu, Q. Zhang, Z. Yan, Q. Xue, Review on electrical discharge plasma technology for wastewater remediation, Chem. Eng. J. 236 (2014) 348–368.
10. J. Steber, P. Wierich, Properties of hydroxyethane diphosphonate affecting its environmental fate: Degradability, sludge adsorption, mobility in soils, and bioconcentration, Chemosphere 15 (1986) 929–945.
11. A.R. Bowers, P. Gaddipati, W.W. Eckenfelder Jr, R.M. Monsen, Treatment of toxic or refractory wastewaters with hydrogen peroxide, Water. Sci. Technol. 21 (1989) 477–486.
12. C. Pulgarín, J. Kiwi, Overview on photocatalytic and electrocatalytic pretreatment of industrial non-biodegradable pollutants and pesticides, Chimia, 50 (1996) 50–55.
13. C.D. Adams, S. Spitzer, R.M. Cowan, Biodegradation of non-ionic surfactants and effects of oxidative pretreatment, J. Environ. Eng. 122 (1996) 477–483.
14. M.T. García, I. Ribosa, T. Guindulain, J. Sánchez-Leal, J. Vives-Rego, Fate and effect of monoalkyl quaternary ammonium surfactants in the aquatic environment, Environ. Pollut. 111 (2001) 169–175.
15. M. Lapertot, C. Pulgarín, P. Fernández-Ibáñez, M.I. Maldonado, L. Pérez-Estrada, I. Oller, W. Gernjak, S. Malato, Enhancing biodegradability of priority substances

(pesticides) by solar photo-Fenton, Water Res. 40 (2006) 1086–1094.
16. R. Muñoz, B. Guieysse, Algal–bacterial processes for the treatment of hazardous contaminants: A review, Water Res. 40 (2006) 2799–2815.
17. M.J. Benotti, R.A. Trenholm, B.J. Vanderford, J.C. Holady, B.D. Stanford, S.A. Snyder, Pharmaceuticals and endocrine disrupting compounds in U.S. drinking water, Environ. Sci. Technol. 43 (2009) 597–603.
18. R. Andreozzi, V. Caprio, R. Marotta, A. Radovnikovic, Ozonation and H_2O_2/UV treatment of clofibric acid in water: a kinetic investigation, J. Hazard. Mater. 103 (2003) 233–246.
19. R. Andreozzi, V. Caprio, R. Marotta, D. Vogna, Paracetamol oxidation from aqueous solutions by means of ozonation and H_2O_2/UV system, Water Res. 37 (2003) 993–1004.
20. L.A. Pérez-Estrada, S. Malato, W. Gernjak, A. Agüera, E.M. Thurman, I. Ferrer, A.R. Fernández-Alba, Photo-Fenton degradation of diclofenac: Identification of main intermediates and degradation pathway, Environ. Sci. Technol. 39 (2005) 8300–8306.
21. T.A. Ternes, M. Meisenheimer, D. McDowell, F. Sacher, H.-J. Brauch, B. Haist-Gulde, G. Preuss, U. Wilme, N. Zulei-Seibert, Removal of pharmaceuticals during drinking water treatment, Environ. Sci. Technol. 36 (2002) 3855–3863.
22. M.-O. Buffle, J. Schumacher, E. Salhi, M. Jekel, U. von Gunten, Measurement of the initial phase of ozone decomposition in water and wastewater by means of a continuous quench-flow system: Application to disinfection and pharmaceutical oxidation, Water Res. 40 (2006) 1884–1894.
23. B. Halling-Sørensen, S.N. Nielsen, P.F. Lanzky, F. Ingerslev, H.C. Lützhøft Holten, S.E. Jørgensen, Occurrence, fate and effects of pharmaceutical substances in the environment—A review, Chemosphere 36 (1998) 357–393.
24. M. Klavarioti, D. Mantzavinos, D. Kassinos, Removal of residual pharmaceuticals from aqueous systems by advanced oxidation processes, Environ. Int. 35 (2009) 402–417.
25. A. Chatzitakis, C. Berberidou, I. Paspaltsis, G. Kyriakou, T. Sklaviadis, I. Poulios, Photocatalytic degradation and drug activity reduction of chloramphenicol, Water Res. 42 (2008) 386–394.
26. F. Méndez-Arriaga, S. Esplugas, J. Giménez, Photocatalytic degradation of non-steroidal anti-inflammatory drugs with TiO_2 and simulated solar irradiation, Water Res. 42 (2008) 585–594.
27. M. Fontecha-Camar, M. Lopez-Ramon, L. Alvarez-Merino, C. Moreno-Castilla. Kinetics of diuron and amitrole adsorption from aqueous solution on activated carbons, J Haz. Mater. 23 (2007) 1242–1247.
28. Y. Xiao, S. Xu, Z. Li, X. An, L. Zhou, Y. Zhang, Q. Fu, Progress of applied research on TiO_2 photocatalysis-membrane separation coupling technology in water and wastewater treatments, Chin. Sci. Bull. 55 (2010) 1345–1353.
29. R. Thiruvenkatachari, S. Vigneswaran, I. S. Moon, A Review on UV/TiO_2 photocatalytic oxidation process, Korean J. Chem. Eng. 25 (2008) 64–72.
30. J. Xu, Y. Ao, M. Chen, D. Fu, C. Yuan, Photocatalytic activity of vanadium-doped

titania-activated carbon composite film under visible light, Thin Solid Films 518 (2010) 4170–4174.
31. M. R. Hoffmann, S. T. Martin, W. Choi, and D. W. Bahnemannt, Environmental Applications of Semiconductor Photocatalysis,Chem. Rev. 95 (1995) 69-96.
32. A. Fujishima, K. Honda, Electrochemical photolysis of water at a semiconductor electrode, Nature 238 (1972) 37–38.
33. T. Ochiai, A. Fujishima, Photoelectrochemical properties of TiO_2 photocatalyst and its applications for environmental purification, J. Photochem. Photobiol. C: Photochem. Rev. 13 (2012) 247–262.
34. U. Shahed, M. Khan*, M. Al-Shahry, B.William Jr. Ingler, Efficient Photochemical Water Splitting by a Chemically Modified n-TiO2, science. 297 (2002) 2243-2245
35. H. P.Jong, S. Kim, and A. J. Bard, Novel Carbon-Doped TiO_2 Nanotube Arrays with High Aspect Ratios for Efficient Solar Water Splitting, Nano Lett., 6 (2006) 24–28.
36. G. Wang, H. Wang, Y. Ling, Y. Tang, X. Yang, R. C. Fitzmorris, C. Wang, J. Z. Zhang and Y. Li, Hydrogen-Treated TiO_2 Nanowire Arrays for Photoelectrochemical Water Splitting, Nano Lett. 11 (2011) 3026–3033.
37. K. Hara, K. Sayama, Y. Ohga, Akira Shinpo, S. Suga and H. Arakawa, A coumarin-derivative dye sensitized nanocrystalline TiO_2 solar cell having a high solar-energy conversion efficiency up to 5.6%, Chem. Commun. 6 (2001) 569-570.
38. M. K. Nazeeruddin , R. Humphry-Baker, P. Liska , and M. Grätzel, Investigation of Sensitizer Adsorption and the Influence of Protons on Current and Voltage of a Dye-Sensitized Nanocrystalline TiO_2 Solar Cell, *J. Phys. Chem. B.* 107 (2003) 8981–8987
39. Ireland, J. C.; Klostermann, P.; Rice, E. W.; Clark, R. M. Appl. Environ. Microbiol. 59 (1993) 1668-1670.
40. Cai, R. X.; Kubota, Y.; Shuin, T.; Sakai, H.; Hashimoto, K; Fujishima, A. Cancer Res. 1992, 52, 2346-2348.
41. M.R. Hoffmann, S.T. Martin, W. Choi, D. W. Bahnemann, Chem. Reviews, 95 (1995) 69–96.
42. J. Schneider, M. Matsuoka, M. Takeuchi, J. Zhang, Y. Horiuchi, M Anpo, D. W. Bahnemann, Chem. Rev. 114 (2014) 9919−9986
43. P. V. Kamat, Photochemistry on nonreactive and reactive (semiconductor) surfaces, Chem. Rev. 93 (1993) 267.
44. M. S. Paul, U. K. Aravind, G. Pramod, C.T. Aravindakumar, Oxidative degradation of fensulfothion by hydroxyl radical in aqueous medium. Chemosphere. 91 (2013) 295–301.
45. R. Sreekanth, KP. Prasanthkumar, MM. Sunil Paul, UK. Aravind, CT. Aravindakumar, Oxidation reactions of 1- and 2-naphthols: an experimental and theoretical study, J. Phys. Chem. A. 117 (2013) 11261–11270.
46. A. L. Stepanov, Applications of ion implantation for modification of TiO2: A Review, Rev. Adv. Mater. Sci. 30 (2012) 150–165
47. R. Asahi, T. Morikawa, T. Ohwaki, K. Aoki, Y. Taga, Visible-light photocatalysis in nitrogen-doped titanium oxides, Science 293 (2001) 269–271.

48. Y. Murakami, B. Kasahara and Y. Nosaka, Photoelectrochemical properties of the sulfur-doped TiO_2 film electrodes: characterization of the doped states by means of the photocurrent measurements, Chem. Lett. 36 (2007) 330–331.
49. S. Rehman, R. Ullah, A.M. Butt, N.D. Gohar, Strategies of making TiO2 and ZnO visible light active, J. Hazard. Mater. 170 (2009) 160–169.
50. B. O'regan, M. Gratzel, A low-cost, high-efficiency solar cell based on dye-sensitized colloidal TiO2 films, Nature. 353(1991) 737–740.
51. T. Tong, J. Zhang, B. Tian, F. Chen, D. He, Preparation of Fe^{3+}-doped tio_2 catalysts by controlled hydrolysis of titanium alkoxide and study on their photocatalytic activity for methyl orange degradation, J. Hazard. Mater. 155 (2008) 572–579.
52. J. F. Zhu, Z. G. Deng, F. Chen, J. L. Zhang, H. J. Chen, M. Anpo, J. Z. Huang, L. Z. Zhang, Hydrothermal doping method for preparation of Cr^{3+}-TiO_2 photocatalysts with concentration gradient distribution of Cr^{3+}, Appl. Catal. B. 62 (2006) 329–335.
53. N. Hamzah, N. M. Nordin, A. H. A. Nadzri, Y. A. Nik, M. B. Kassim, M. A. Yarmo, Enhanced activity of Ru/TiO_2 catalyst using bisupport, bentonite-TiO_2 for hydrogenolysis of glycerol in aqueous media, Appl. Catal. A. 419−420 (2012) 133–141.
54. S. Yuan, Y. Chen, L. Y. Shi, J. H. Fang, J. P. Zhang, J. L. Zhang, H. Yamashita, Synthesis and characterization of Ce-doped mesoporous anatase with long-range ordered mesostructure, Mater. Lett. 61 (2007) 4283–4286.
55. H. T. Gao, W. C. Liu, B. Lu, F. F. Liu, Photocatalytic Activity of La, Y Co-Doped tio_2 Nanoparticles Synthesized by Ultrasonic Assisted Sol–Gel Method, J. Nanosci. Nanotechnol. 12 (2012) 3959–3965.
56. H. B. Liu, Y. M. Wu, J. L. Zhang, A new approach toward carbon-modified vanadium-doped titanium dioxide photocatalysts, ACS Appl. Mater. Interfaces. 3 (2011) 1757–1764.
57. W. Y. Choi, A. Termin, M. R. Hoffmann, The role of metal ion dopants in quantum-sized TiO_2: correlation between photoreactivity and charge carrier recombination dynamics, J. Phys. Chem. 98 (1994) 13669–13679.
58. J. Zhang, Y. Wu, M. Xing, S. A. K. Leghari, S. Sajjad, Development of modified N doped TiO_2 photocatalyst with metals, nonmetals and metal oxides, Energy Environ. Sci. 3 (2010) 715–726.
59. C. D. Valentin, G. Pacchioni, A. Selloni, S. Livraghi, E. Giamello, Characterization of paramagnetic species in N-doped TiO_2 powders by EPR spectroscopy and DFT calculations, J. Phys. Chem. B. 109 (2005) 11414–11419.
60. S. Sato, R. Nakamura, S. Abe, Visible-light sensitization of TiO_2 photocatalysts by wet-method N doping, Appl. Catal. A: Gen. 284 (2005) 131–137.
61. H. Kisch, S. Sakthievel, M. Janczarek, D. Mitoraj, A low-band gap, nitrogen-modified titania visible-light photocatalyst, J. Phys. Chem. C. 109 (2007) 11445–11449.
62. M. Batzill, E. H. Morales, U. Diebold, Surface studies of nitrogen implanted TiO_2, Chem. Phys. 339 (2007) 36–43.
63. K. Yamanaka, T. Morikawa, Charge-carrier dynamics in nitrogen-doped TiO_2 powder studied by femtosecond time-resolved diffuse reflectance spectroscopy, J.

Phys. Chem. C. 116 (2012) 1286–1292.
64. G. Barolo, S. Livraghi, M. Chiesa, M. C. Paganini, and E. Giamello, Mechanism of the photoactivity under visible light of N-doped titanium dioxide. Charge carriers migration in irradiated N-TiO_2 investigated by electron paramagnetic resonance. J. Phys. Chem. C. 116 (2012) 20887–20894.
65. S. Yamanaka, Y. Inoue, M. Hattori, F. Okumura, M. Yoshikawa, Preparation and properties of clays pillared with SiO_2-TiO_2 sol particles. Bull. Chem. Soc. Jpn. 65 (1992) 2494–2500.
66. Y. Kameshima, Y. Tamura, A. Nakajima, K. Okada, Preparation and properties of TiO_2/montmorillonite composites, Applied Clay Science. 45 (2009) 20–23.
67. L. Pauling, The structure of the chlorites, Proc Natl Acad Sci USA. 16 (1930) 578–582.
68. K. G. Bhattacharyya, S. S. Gupta, Adsorption of a few heavy metals on natural and modified kaolinite and montmorillonite: A review, Adv. Colloid. Interfac. 140 (2008) 114–131.
69. S. Ng and J. Plank, Interaction mechanisms between Na montmorillonite clay and MPEG-based polycarboxylate superplasticizers, Cem. Concr. Res. 42 (2012) 847–854.
70. Kaneko, T., Shimotsuma, H., Kajikawa, M. et al., Synthesis and photocatalytic activity of titania pillared clays, J. Porous. Mat.8 (2001) 295–301.
71. C. Ooka, H. Yoshida, M. Horio, K. Suzuki, T. Hattori, Adsorptive and photocatalytic performance of TiO_2 pillared montmorillonite in degradation of endocrine disruptors having different hydrophobicity, Applied Catalysis B: Environmental. 41 (2003) 313–321.
72. D. Kibanova, M. Sleiman, J. Cervini-Silva, H. Destaillats, Adsorption and photocatalytic oxidation of formaldehyde on a clay-TiO_2 composite, Journal of Hazardous Materials. 211–212 (2012) 233–239.
73. C. Ooka, H. Yoshida, K. Suzuki, T. Hattori, Highly hydrophobic TiO_2 pillared clay for photocatalytic degradation of organic compounds in water, Micropor. Mesopor. Mater. 67 (2004) 143–150.
74. Y. Kameshima, Y. Tamura, A. Nakajima, K. Okada, Preparation and properties of TiO2/montmorillonite composites, Applied Clay Science. 45 (2009) 20–23.
75. Prieto-Mahaney, O.O., Murakami, N., Abe, R., Ohtani, B., 2009. Correlation between photocatalytic activities and structural and physical properties of titanium(iv) oxide powders. Chemistry Letters. 38 (3), 238–239.
76. G. Zhang, X. Ding, Y Hu, B. Huang, X. Zhang, X. Qin, J. Zhou, and J. Xie, Photocatalytic Degradation of 4BS Dye by N,S-Codoped-TiO_2 pillared montmorillonite photocatalysts under visible-light irradiation, J. Phys. Chem. C. 112 (2008) 17994–17997.
77. K. Chen, J. Li, W. Wang, Y. Zhang, X. Wang, H. Su, The preparation of vanadium-doped TiO_2-montmorillonite nanocomposites and the photodegradation of sulforhodamine B under visible light irradiation, Applied Surface Science. 257 (2011) 7276–7285.
78. R. Sasai, R. Watanabe T. Yamada, Preparation and characterization of titania-and

organo-pillared clay hybrid photocatalysts capable of oxidizing aqueous bisphenol A under visible light, Applied Clay Science. 93–94 (2014) 72-77.
79. J. Zhang, L. Zhang, J. Lv, S. Zhou, H. Chen, Y. Zhao, X. Wang, Exceptional visible-light-induced photocatalytic activity of attapulgite-BiOBr-TiO_2 nanocomposites, Applied Clay Science. 90 (2014) 135–140.

Chapter 2 Preparation and characterization of N-TiO_2/montmorillonite composite

2.1 Introduction

TiO_2 is a wide bandgap semiconductor (e.g., anatase, 3.2 eV) which has very strong oxidizability on the decomposition of organic materials. However, wide bandgap always requires high photon energy (no less than the bandgap energy) for photoexcitation of electrons and holes[1]. Thereby, TiO_2 is effective only under UV light irradiation, in other words, only a few photoexcited electrons and holes can be arose under solar light of which major constituent is the visible light. As mentioned in the mechanisms of TiO_2 photocatalysis, the amount of photoexcited electrons and holes participating in the photoredox reaction makes a great effect on improving the photocatalytic activity of TiO_2[2]. Therefore, how to produce available photoexcited electrons and holes under visible light irradiation is the key point to visible light responsive TiO_2

Nitrogen doping is an outstanding method to enhance photocatalytic activity by modification of the TiO_2 bandgap. The nitrogen anions introduced by nitrogen doping arise two different chemical states, either substitutional N or interstitial N[3-7]. In both cases, an isolated N 2p midgap generates above the top of the valence band, reducing the bandgap energy of TiO_2 (shown in scheme 3.1). Thus, photoexcitation of electrons is available under visible light irradiation, which has relatively lower photon energy. On the other hand, nitrogen doping results in oxygen vacancies act as recombination centers of photoexcited electrons and holes[8]. In particular, excessive nitrogen amount leads to inhibition of photocatalytic activity. Thus, an appropriate nitrogen content in N-TiO_2 play an important role in the improvement of photocatalytic activity of TiO_2. Another essential factor to nitrogen dope TiO_2 is calcination temperature. With increasing the calcination temperature, particle size usually increases due to the agglomeration of small particles[9]. It is also reported that the amount of introduced nitrogen atom in nitrogen doped TiO_2 may reduce under high calcination temperature, decreasing the photocatalytic activity of nitrogen doped TiO_2[10].

In this chapter, the NTM composite was prepared via sol-gel method. The property of NTM composite was characterized. The conditions to prepare NTM composite, nitrogen content and calcination temperature, were discussed via evaluation of photocatalytic activity.

2.2 Experimental procedure

2.2.1 Preparation of N-TiO_2/montmorillonite composite

Materials

Sodium-montmorillonite from Aderazawa, Yamagata, Japan (Kunipia-F, Kunimine) and titanium tetra iso-propoxide(TTIP, $Ti(OC_3H_7)_4$, Kanto Chemical) were used as the initial materials. The cation exchange capacity (CEC_{Clay}) of Montmorillonite was 1.15 m eq/g. Urea ($CO(NH_2)_2$, Kanto Chemical) was used as a nitrogen source for nitrogen doping.

Sample preparation

The aqueous dispersion was prepared by dispersing 1.0 g of montmorillonite into 100 mL water, stirring for 24 hours. The initial aqueous solution was prepared by dissolving 13.07 g of TTIP and certain amount of urea into 30 ml of ethanol, keeping the N / Ti ratio as 0.5, 1, 1.5, 2 and 3. The solution was then added to 1 M HCl solution dropwise, stirring vigorously for 3 hours at room temperature (25°C). The stirred solution was introduced into montmorillonite dispersion with vigorous stirring and keeping stirring for another 3 hours at room temperature. The wet cake-like precipitate was produced by centrifuging and washing. After drying at 120 °C, the produced solid was milled, and then calcined at 250 °C for 2 hours at a rate of 5 °C/min of temperature shift. The prepared sample was named at NTM-0.5, NTM-1.0, NTM-1.5, NTM-2.0 and NTM-3.0.

Another series of sample were prepared via the similar method, except keeping the N / Ti ratio as 1.5 and calcined at 250°C, 300°C, 350°C and 400°C. The prepared sample was named at NTM-250, NTM-300, NTM-350 and NTM-400.

2.2.2 Preparation of N-doped TiO_2 sol

Materials

Titanium tetra iso-propoxide(TTIP, $Ti(OC_3H_7)_4$, Kanto Chemical) were used as the initial materials. Urea($CO(NH_2)_2$, Kanto Chemical) was used as a nitrogen source for nitrogen doping.

Sample preparation

The NH_4^+ solution was prepared by dissolving 13.07 g of TTIP into 30 ml of ethanol, keeping the N / Ti ratio at 1.5. The solution was added to 1 M HCl solution dropwise, stirring vigorously for 3 hours at room temperature (25°C). Then, the stirred solution was kept in still standing for 12 h. The precipitate was produced after washing and centrifuging. The produced solid was dried at 120 °C and milled, and then, calcination was carried out at the sited temperature at 250°C, 300°C, 350°C and 400°C, for 2 hours at a rate of 5 °C/min of temperature shift. The prepared samples were named as NT-250, NT-300, NT-350 and NT-400.

2.2.3 Characterization

X-ray diffraction(XRD) patterns were recorded by using Cu Kα radiation (λ = 1.5418 Å) on a Rigaku Rint2100 operation at 40 kV and 30 mA with 0.25° divergence slit, 0.5° antiscatter slit, between 1 and 60° (2θ). The crystallite sizes of TiO_2 particles were calculated by Scherrer's equation for the (*101*) reflection at about 2θ = 25°. UV-vis diffuse reflectance spectra were measured at room temperature in air on a Shimadzu UV-2450 photometer over the range 200 to 800 nm, while $BaSO_4$ was used as a

reference. Chemical contents of each sample were analyzed by energy dispersive spectra (EDS, JED-2300) measurements which was equipped on scanning electron microscopy (SEM, JSM-6380A). Carbon content was recorded by thermal analysis (TG-DTA, TG8120/SH) at a heating rate of 10°C min^{-1} under air using R-Al_2O_3 as the standard material.

2.2.4 Photocatalytic activity

The photocatalytic activity of NTM was evaluated by photodecomposition of BPA in aqueous solution. A catalyst loading of 100 mg per 100 mL of solution was used. The initial concentration of BPA was 10 ppm. The suspension contained in the Pyrex glass beaker was placed in a thermostatic water bath at constant 25 °C for 1 h of magnetic stirring in the dark to attain an adsorption–desorption equilibrium of BPA. Subsequently, the photodecomposition of BPA was performed under visible light irradiation by using a Xe lamp(BA-X502) equipped with both UV filter and IR filter to select the required wavelength (420 nm < λ < 1200 nm). The intensity of the light source was fixed at 10 mW/cm^2 and the vertical distance from the lamp to the surface of suspension was also fixed at about 20 cm. The concentration of BPA was analyzed by using HPLC (Shimadzu LC-20AT) instrument equipped with a UV-vis detector and an C18 separation column(5 μm, 150 × 4.6 mm). The elution was monitored at 254 nm. The mobile phase was a mixture of acetonitrile and water (50/50, v/v), which was pumped at a flow rate of 1.0 mL min^{-1}.

Table 2.1 Conditions of photodecomposition

Concentration of BPA	10 ppm
Solution volume	200 mL
Temperature	25°C
Catalyst dosage	0.1 g（1.0 g/L）
Light source	300 W Xe lamp
Irradiation intensity	10 mW/cm^2（420 nm < λ < 1200 nm）

2.3 Results and discussion

2.3.1 Characterization

The NTM composites prepared with various N / Ti ratio (from 0.5 to 3) were analyzed by XRD and the results are shown in Fig. 2.1. The NTM composites exhibit very similar XRD patterns, which indicated the approximately same structure of each composite even though the nitrogen content is different. The distinct broadening 001 peak and the unchanged 101 peak indicated the disordered structure including randomly agglomerated TiO_2 particles and montmorillonite layers. The TiO_2 particles in all the composites were observed as only anatase phase (at 2θ = 25°, 37°, 48°, 54°). The XRD pattern of NTM composites prepared under various calcination temperatures (from 150 to 400°C) are shown in Fig. 2.2. All the samples show a very similar XRD pattern. By increasing the calcination temperature, however, the 001 peak gradually shift to higher angle. This tendency indicated the decreases of basal spacing, resulted from the dehydration of TiO_2 particles in the interlayers of montmorillnite. In addition, the anatase peak became sharper gradually, indicating the crystallinity of TiO_2 increased with increasing the calcination temperature.

The UV-vis diffuse reflection spectra of the NTM-0.5, NTM-1.0, NTM-1.5, NTM-2.0 and NTM-3.0 samples are shown in Fig. 2.3. All samples exhibited a light ivory color. The absorbance of the samples increased gradually with the N / Ti ratio increasing. This color changing was attributed to the fact that nitrogen anions introduced in TiO_2 crystalline by nitrogen doping act as chromophoric center*[4]*. In addition, by increasing

the N / Ti ratio, more organics might be introduced into the NTM composite due to a heavy dosage of nitrogen source. These organics may result in incomplete combustion, thus leading to color increases over the visible light region. In order to better study the effect of calcination temperature to NTM composite, the nitrogen doped TiO_2 was prepared via same method but without montmorillonite. The results(as shown in Fig. 2.4) of NT samples are similar to that of NTM samples. The The UV-vis diffuse reflection spectra of the NTM composites calcined at various temperatures are shown in Fig. 2.5. The color of the samples enhanced gradually by raising the calcination temperature, but stop to decrease when the calcination temperature over 350°C. The decreased absorbance was attributed to nitrogen loss*[10]*. During the calcination at high temperature, large amount of ammonia could be desorbed before nitrogen introduced into the TiO_2 lattice. The UV-vis diffuse reflection spectra of NT samples calcined at various temperatures are shown in Fig. 2.6. The results are well corresponding to that of NTM composite and similar to that reported in relative papers*[5,10]*.

The chemical content of the NTM-0.5, NTM-1.0, NTM-1.5, NTM-2.0 and NTM-3.0 samples are shown in Fig. 2.7. From the result, with increasing the nitrogen content, the Al / Si ratio in each sample maintained, indicating that the unchanged alumina-silica layered structure of montmorillonite. However, the TiO_2 content decreased to some extent with increasing the nitrogen content, indicating that heavy nitrogen doping result in low TiO2 content which may reduce the photocatalytic activity.

SEM images of the NTM composites calcined at 250°C and 400°C are shown in Fig. 2.8. As can be seen from SEM image, the particle size of the sample 250°C is smaller than that of the sample calcined at 400°C, which indicated that high calcination temperature lead to agglomeration*[11,12]* of the sample particles.

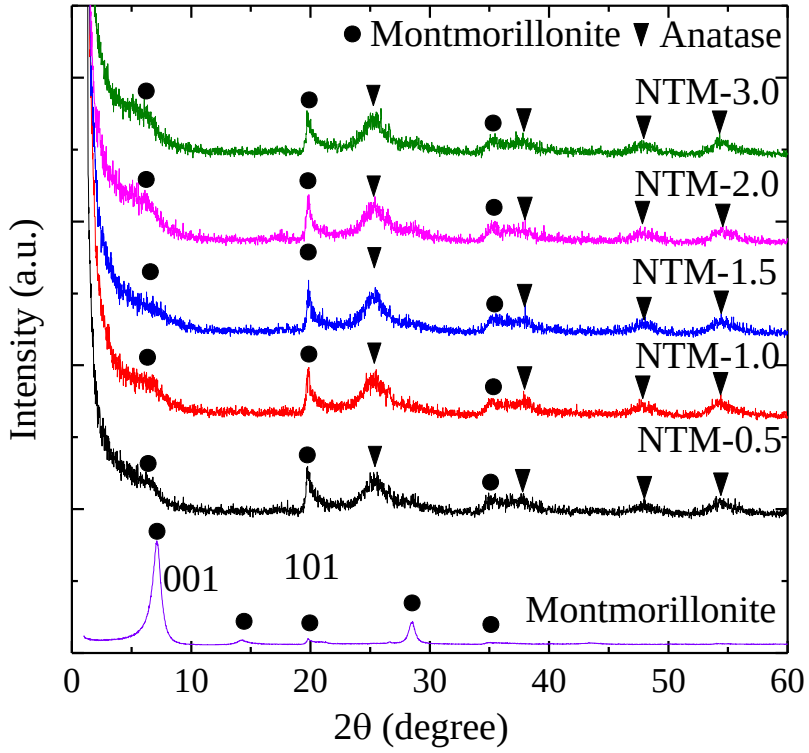

Fig. 2.1 XRD patterns of the NTM composites prepared with various N / Ti ratio.

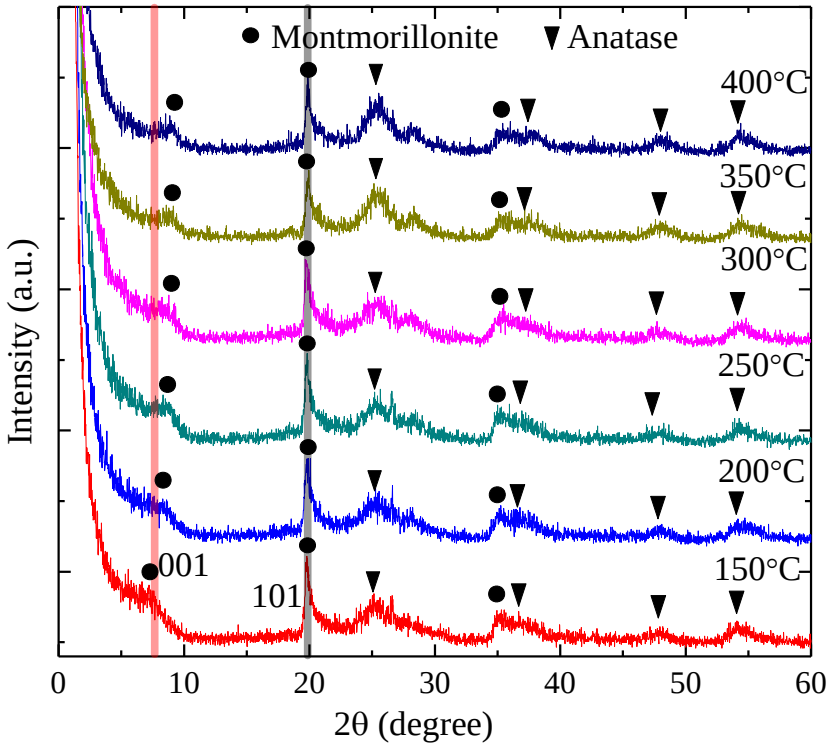

Fig. 2.2 XRD patterns of the NTM composites calcined at various temperatures

.

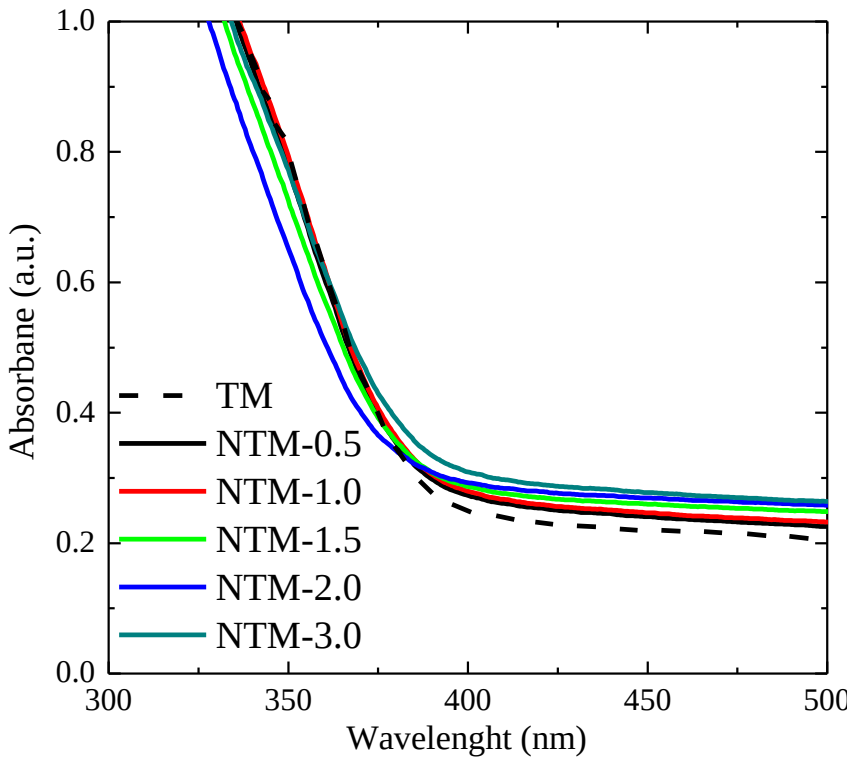

Fig. 2.3 UV-vis diffuse reflection spectra of the NTM composites prepared with various N / Ti ratio.

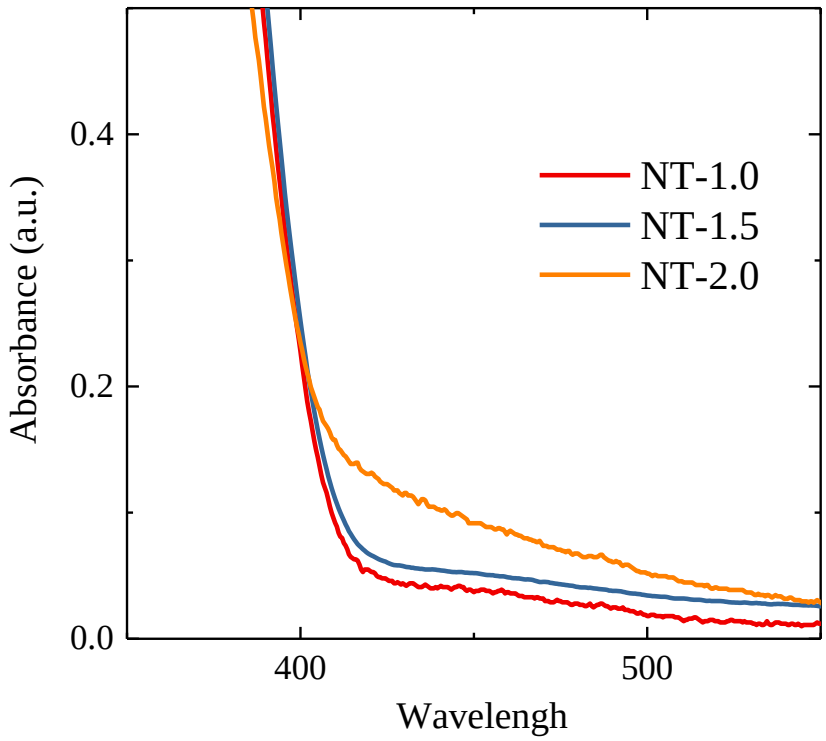

Fig. 2.4 UV-vis diffuse reflection spectra of the NT-1.0, NT-1.5, NT-2.0 samples.

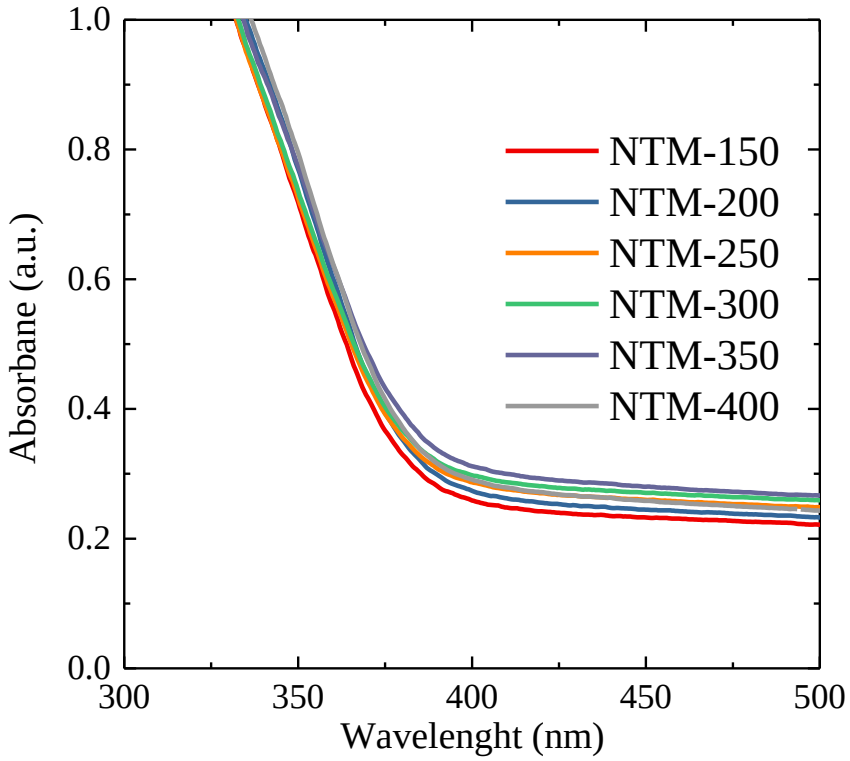

Fig. 2.5 UV-vis diffuse reflection spectra of the NTM composites calcined at various temperatures.

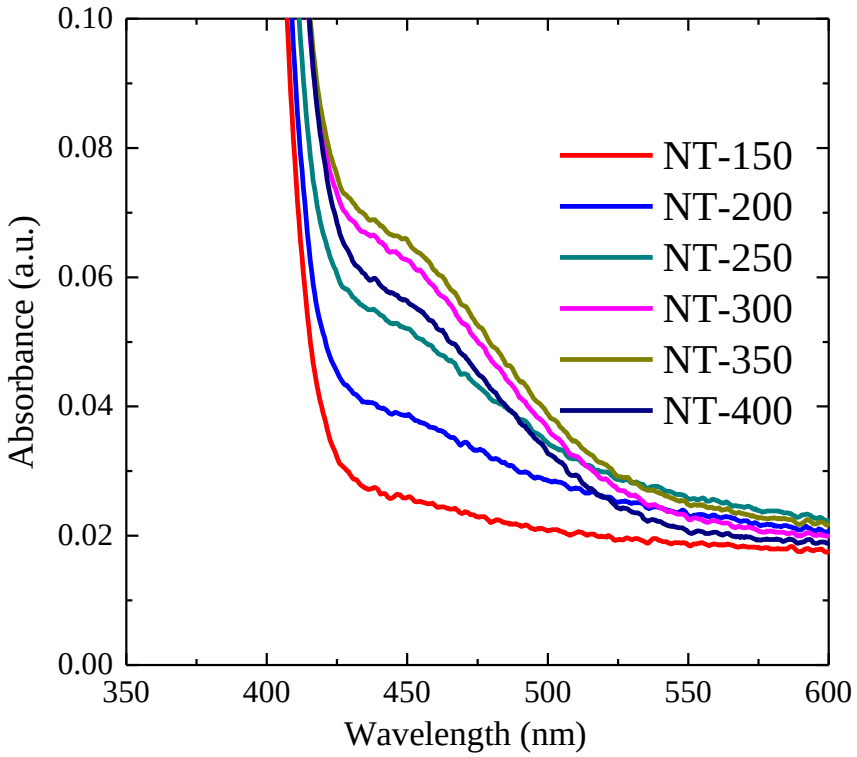

Fig. 2.6 UV-vis diffuse reflection spectra of nitrogen doped TiO_2 calcined at various temperatures.

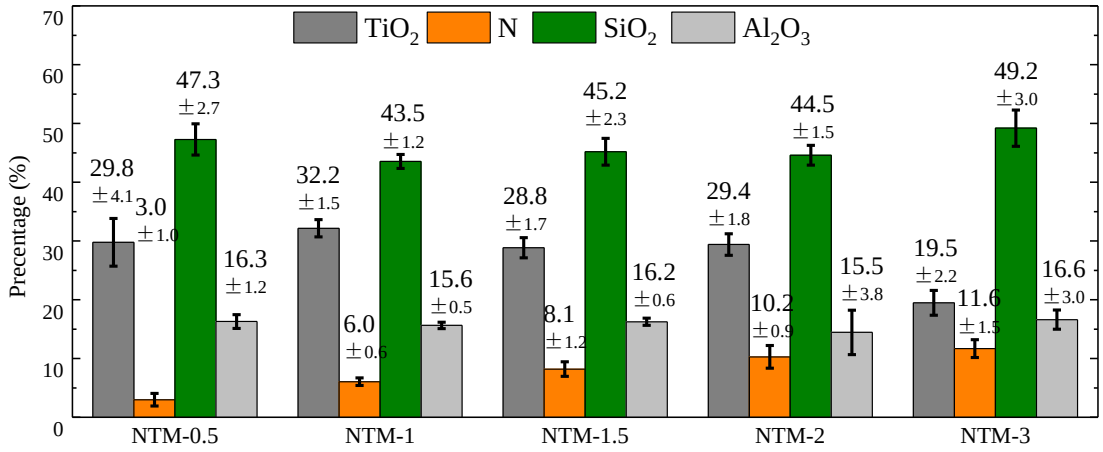

Fig. 2.7 Chemical contents of the NTM-0.5, NTM-1.0, NTM-1.5, NTM-2.0 and NTM-3.0 composite

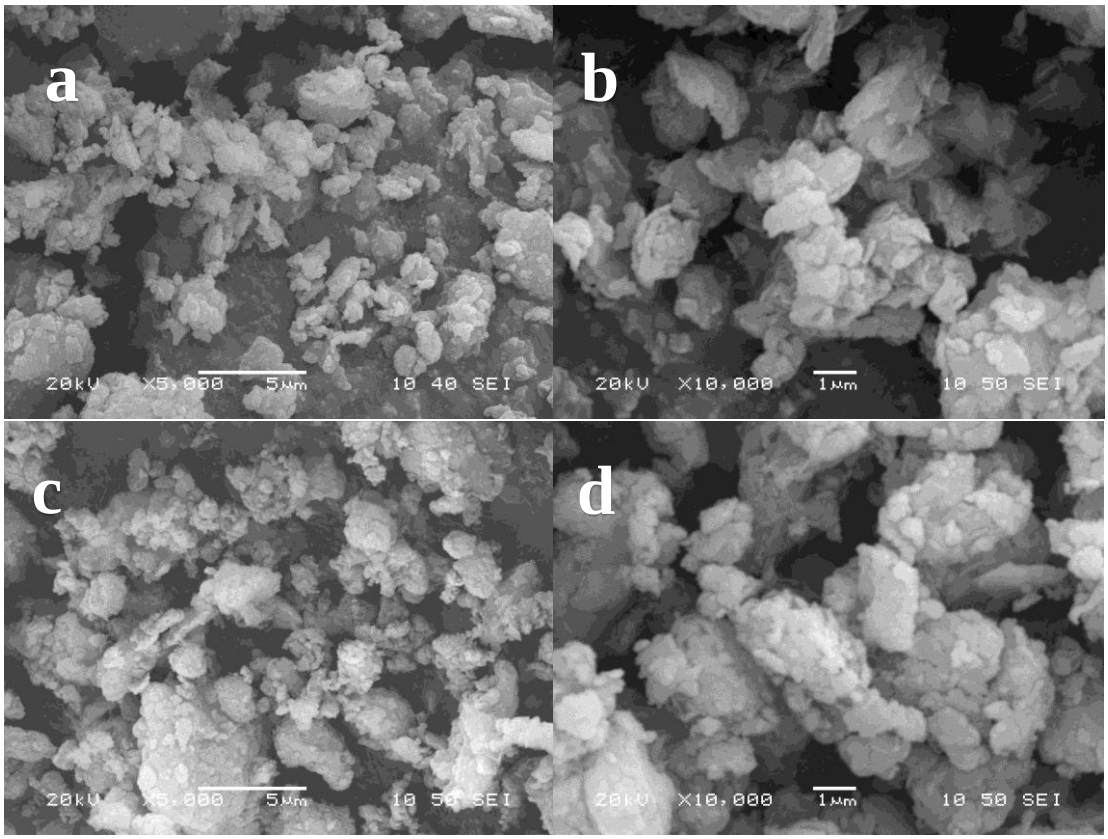

Fig. 2.8 SEM image of the NTM composites calcined at 250°C, (a) ×5000, (b) ×10000 and at 400°C, (c) ×5000 (d) ×10000.

2.3.2 Effect of N / Ti ratio on photocatalytic activity

The removal rate of BPA in the absence of irradiation or without a sample was carried out and the result is shown in Fig. 2.9. According to these results, the removal rate of BPA in the absence of irradiation or without a catalyst was very low. Due to the polarity of BPA is extremely weak, unlike other organics; BPA cannot be greatly adsorbed by NTM composites. In addition, the adsorption behavior of all kinds of NTM composites was almost similar and in each case a very low adsorption was observed. Therefore, it should be noticed that the role of adsorption is almost negligible while considering the decomposition of BPA becomes more important.

The decomposition rate of BPA by using NTM composite with various N / Ti ratio are shown in Fig. 2.10. Apparently, the results indicated that the nitrogen content in TiO_2 makes a great effect on photocatalytic activity of the catalyst. The decomposition rate of BPA increased following the N / Ti ratio increasing. When the N / Ti ratio was 1.5, the sample exhibited the highest decomposition rate. Although the actual nitrogen content still kept on increasing when further raised the N / Ti ratio over 1.5, the decomposition rate stops to decrease on the contrary. This result indicated that nitrogen doping on one hand can effectively improve the visible light response of TiO_2, on the other hand, high doping amount of nitrogen results in a large number of oxygen vacancies. These defects of crystalline in TiO_2 may act as recombination centers*[13]* of photoexcited electrons and positive holes, greatly decreasing the photocatalytic activity. In addition, the actual TiO_2 content is also an important factor to the decomposition rate. It was observed that increasing the N / Ti ratio result in the decrease of actual TiO_2 content. Consequently, it was found that the optimum N / Ti ratio to the maximum decomposition rate of BPA was 1.5.

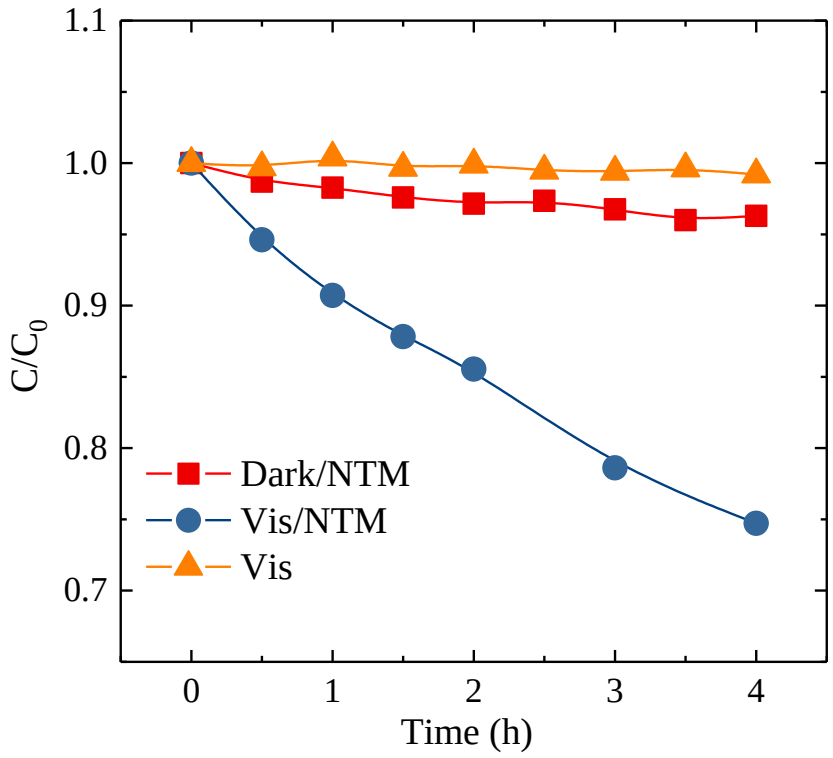

Fig. 2.9 Decomposition rate of BPA in the absence of irradiation and that without a sample.

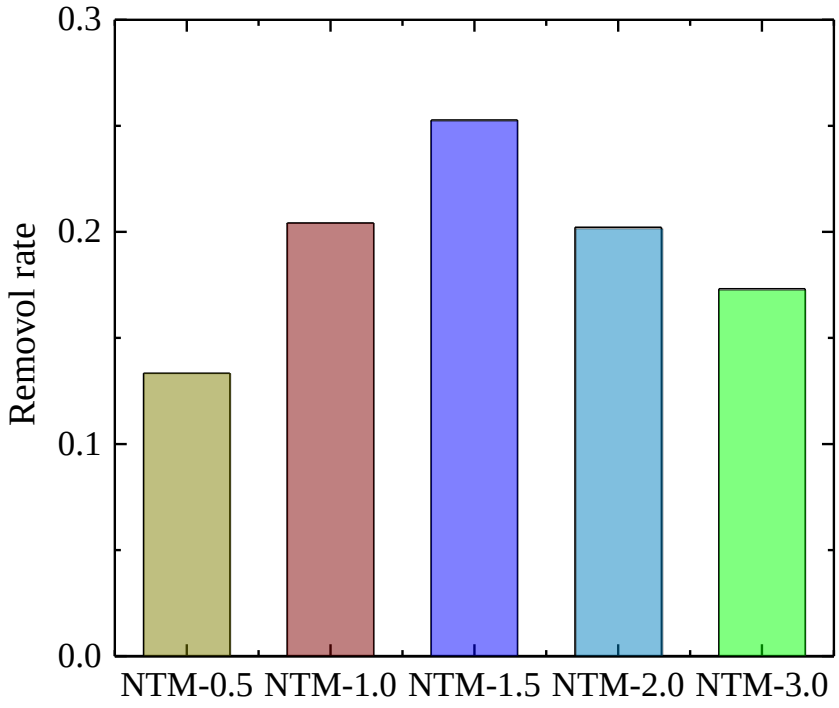

Fig. 2.10 Decomposition rate of BPA by using NTM composite with various N / Ti ratio

2.3.3 Effect of heat treatment on photocatalytic activity

The decomposition rate of BPA by using NTM composite calcined at various temperatures are shown in Fig. 2.11. With raising the calcination temperature, the decomposition rate of BPA increase until the calcination temperature reached to 250°C. When further increasing calcination temperature, the decomposition rate of BPA started to decrease greatly. The optimum calcination temperature for highest decomposition rate of BPA was found to be as 250°C, not quite corresponding to other research*[14-17]* related to N doped TiO_2 catalyst, which reported that the optimum calcination temperatures were 400°C or higher temperature due to the fact that the TiO_2 particles have larger specific surface area or higher crystallinity of anatase or both. In the case of our research, the NTM composite, however, when the calcination temperature over 250°C, the basal spacing of montmorillonite decreased due to the dehydration of the TiO_2 particles, resulting in great decreased photocatalytic activity of NTM composite. Apparently, the advantages resulted from high calcination temperature could not overcome the concomitant negative effect from the dehydration of the TiO_2 particles.

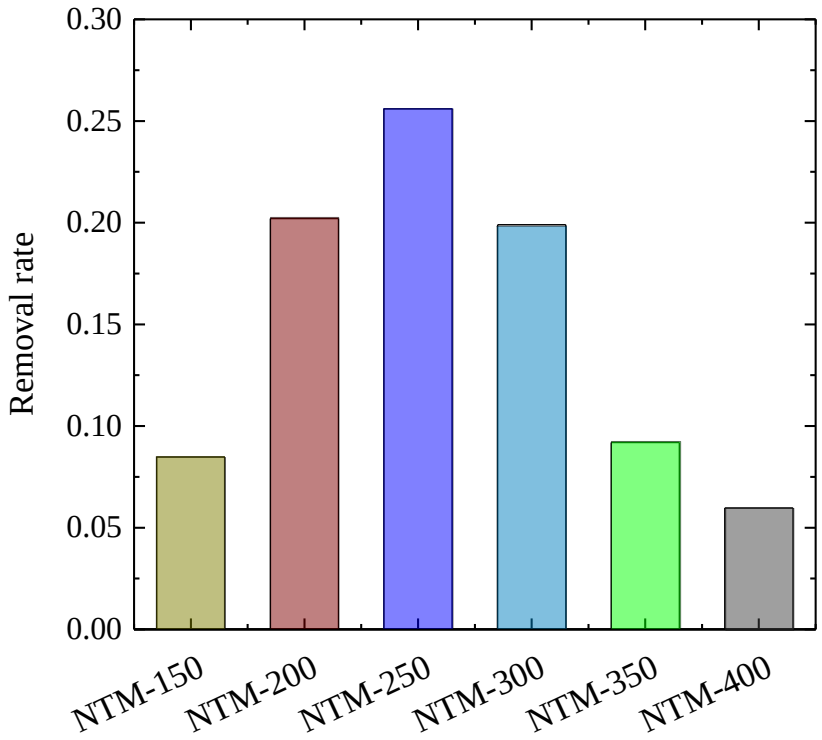

Fig. 2.11 Decomposition rate of BPA by using NTM composite calcined at various temperatures.

2.4 Conclusion

According to the characterization results, the phase of the intercalated TiO_2 particles in both cases of NTM samples (the sample with various N / Ti ratio and the samples with various calcination temperature) was identified as anatase. With increasing the N / Ti ratio of the NTM composite, the absorbance around 400 to 600 nm enhanced gradually due to the fact that nitrogen introduced in the TiO_2 crystalline act as chromophoric center. When raise the calcination temperature, the absorbance enhanced gradually, but stop to decrease over 350°C. The decreased absorbance was attributed to the fact that calcination leads to nitrogen loss at high temperature. The decomposition of BPA was carried out for evaluation of photocatalytic activity. From the results, it is worth to notice that the decomposition of BPA in the absence of irradiation or without a photocatalyst was almost negligible. Consequently, the adsorption behavior of BPA is almost negligible while the discussion on photodecomposition of BPA becomes more important. When the N / Ti ratio of the NTM composite was increased, the decomposition rate of BPA increased with the N / Ti ratio up to 1.5, and then became to decrease gradually due to the fact that high doping amount leads to a large number of oxygen vacancies. These defects of crystalline in TiO_2 may act as recombination centers of photoexcited electrons and positive holes, greatly decreasing the photocatalytic activity. The optimum calcination temperature was 250°C. With further raising the calcination temperature, the photocatalytic activity decreased due to the dehydration of the TiO_2 particles.

2.5 Reference

1. K, Hashimoto, H Irie and A, Fujishima. TiO2 Photocatalysis: A historical overview and future prospects. Jpn. J. Appl. Phys. 44 (2005) 8269–8285.
2. J. Schneider, M. Matsuoka, M. Takeuchi, J. Zhang, Y. Horiuchi,M Anpo, and D. W. Bahnemann. Understanding TiO_2 photocatalysis: mechanisms and materials Chem. Rev. 114 (2014) 9919−9986.
3. C. D. Valentin, G. Pacchioni, A. Selloni, S. Livraghi, E. Giamello, Characterization of paramagnetic species in N-doped TiO_2 powders by EPR spectroscopy and DFT calculations, J. Phys. Chem. B. 109 (2005) 11414–11419.
4. S. Sato, R. Nakamura, S. Abe, Visible-light sensitization of TiO_2 photocatalysts by wet-method N doping, Appl. Catal. A: Gen. 284 (2005) 131–137.
5. S. Sakthivel, H. Kisch, Photocatalytic and photoelectrochemical properties of nitrogen-doped titanium dioxide, Chem. Phys. Chem. 4 (2003) 487–490.
6. H. Kisch, S. Sakthievel, M. Janczarek, D. Mitoraj, A low-band gap, nitrogen-modified titania visible-light photocatalyst, J. Phys. Chem. C. 109 (2007) 11445–11449.
7. G. Barolo, S. Livraghi, M. Chiesa, M. C. Paganini, and E. Giamello, Mechanism of the photoactivity under visible light of N-doped titanium dioxide. Charge carriers migration in irradiated N-TiO_2 investigated by electron paramagnetic resonance. J. Phys. Chem. C. 116 (2012) 20887–20894.
8. H. Irie, Y. Watanabe, and K. Hashimoto, Nitrogen-concentration dependence on photocatalytic Activity of $TiO_{2-x}N_x$ powders, J. Phys. Chem. B. 107 (2003) 5483-5486.
9. T. Ohno, T. Mitsui, M. Matsumura. Photocatalytic activity of S-doped TiO_2 photocatalyst under visible Light. M. Chem. Lett. 3(2003) 364−365.
10. M. Sathish, B. Viswanathan, R. P. Viswanath, C. S. Gopinath. Synthesis, characterization, electronic structure, and photocatalytic activity of nitrogen-doped TiO_2 nanocatalyst. Chem. Mater. 17(2005) 6349−6353.
11. G. Li, L. Lv, H. Fan, J. Ma, Y. Li, Y. Wan, X. S. Zhao. Effect of the agglomeration of TiO_2 nanoparticles on their photocatalytic performance in the aqueous phase. Journal of Colloid and Interface Science. 348 (2010) 342−347.
12. K. Fischer, A. Gawel, D. Rosen, M. Krause, A. A. Latif, J. Griebel, A. Prager, A. Schulze. Low-temperature synthesis of anatase/rutile/brookite TiO_2 nanoparticles on a polymer membrane for photocatalysis.7 (2017) doi: 10.3390/catal7070209.
13. H. Irie, Y. Watanabe, and K. Hashimoto, Nitrogen-concentration dependence on photocatalytic Activity of TiO_2-xNx powders, J. Phys. Chem. B. 107 (2003) 5483-5486.
14. Ye Cong, Jinlong Zhang, Feng Chen, Masakazu Anpo. Synthesis and characterization of nitrogen-doped TiO_2 nanophotocatalyst with high visible light activity. J. Phys. Chem. C. 111 (2007) 6976-6982.
15. T. Ihara, M. Miyoshi, Y. Iriyama, O. Matsumoto, S. Sugihara. Visible-light active titanium oxide photocatalyst realized by an oxygen-deficient structure and

by nitrogen doping. Applied Catalysis B: Environmental. 42 (2003) 403–409.
16. S. Sato, R. Nakamura, S. Abe, Visible-light sensitization of TiO_2 photocatalysts by wet-method N doping, Appl. Catal. A: Gen. 284 (2005) 131–137.
17. M. Sathish, B. Viswanathan, R. P. Viswanath, C. S. Gopinath, Synthesis, characterization, electronic structure, and photocatalytic activity of nitrogen-doped TiO_2 nanocatalyst. Chem. Mater. 17 (2005) 6349-6353.

Chapter 3. Preparation and characterization of carbon deposited N-TiO_2/montmorillonite composite

3.1 Introduction

In photocatalysis over TiO_2 particles, photoexcited electrons and positive holes separate and react with the species adsorbed on the surface TiO_2 particles, resulting in oxidation and reduction reactions, respectively. Longer lifetimes of these photoexcited charge carriers before they recombine with each other result in higher photocatalytic activity[1,2]. Thereby, the lifetime of photoexcited electrons and positive holes plays a very important role in the photocatalysis. Nitrogen doping can greatly enhance the photocatalytic activity by reducing the bandgap energy of TiO_2, thus resulting in visible light responsibility[3-6]. On the other hand, the O vacancies induced by nitrogen anions act as recombination centers of photoexcited electrons and positive holes, decreasing the lifetime of photoexcited electrons and positive holes to some extent[7]. Especially in the case of small particles, e.g., the TiO_2 particles in NTM composite, of which size is usually quite small(less than 2nm)[8-11]. The recombination is more likely to occur due to the fact that the photoexcited electron and hole pairs cannot be sufficiently separated from each other in the limited spatial region. Therefore, how to effectively facilitate the separation of photoexcited electrons and positive holes is one of the determining factors to improve photocatalytic activity.

Carbonaceous materials exhibit excellent chemical and electrical properties. The utilization of carbonaceous nanomaterials to improve the photocatalytic activity of TiO_2 has attracted increasing attention. It is reported that carbon modified TiO_2 exhibits improved photocatalytic activity due to greater retardation to the recombination of photoexcited electrons and positive holes[12-14]. Some research have revealed that the photocatalytic activity could be enhanced by carbonaceous species after incomplete calcination procedures[15-17]. It may be suggested a new modification method for TiO_2 catalyst, which is easy to operate under lower calcination temperature in addition to remarkable effect. By now, it is rarely reported that TiO_2/clay composites, treated with carbon modification. Thereby, to effectively facilitate the separation of photoexcited

electrons and positive holes, it is interesting to study carbon deposited N-doped TiO_2/montmorillonite.

In this chapter, the dried N-doped TiO_2/montmorillonite colloidal was treated with carbon modification by using ethanol, one of the most common carbohydrates, as a carbon source. During this process, carbonaceous species can be deposited on the surface of TiO_2 particles (as shown in Fig. 3.1), leading to effective electron transfer from TiO_2 particles to carbonaceous species. The characterization and photocatalytic activity of carbon deposited N-doped TiO_2/montmorillonite(CNTM) composite were studied. In addition, the effect of carbon content on photocatalytic activity was discussed.

Fig. 3.1 Carbon diposition of N-doped TiO_2/montmorillonite composite

3.2 Experimental procedure

3.2.1 Preparation of CNTM composite

Materials

Sodium-montmorillonite from Aderazawa, Yamagata, Japan(Kunipia-F, Kunimine) and titanium tetra iso-propoxide(TTIP, $Ti(OC_3H_7)_4$, Kanto Chemical) were used as the initial materials. The cation exchange capacity (CEC_{Clay}) of Montmorillonite was 1.15 meq/g. Urea($CO(NH_2)_2$, Kanto Chemical) was used as a nitrogen source for nitrogen doping.

Sample preparation

The aqueous dispersion was prepared by dispersing 1.0 g of montmorillonite into 100 mL water, and stirred for 24 hours. The initial aqueous solution was prepared by dissolving 13.07 g of TTIP and 1.35 g urea into 30 ml of ethanol, keeping the N / Ti = 1.0. The solution was then added to 1 M HCl solution dropwise, keeping vigorous stirring for 3 hours at room temperature (25°C). The solution was then introduced into montmorillonite dispersion with vigorous stirring and keeping stirring for another 3 hours at room temperature. The wet cake-like colloidal was produced by washing until pH reaching up to 6 and centrifuging several times. After drying at 120°C, the solid was milled, and then transferred into alumina crucible. Ethanol was added into the solid at the dosage of 0.5, 1, 2 and 3 mL/g composite. The samples was named as CNTM-0.5, CNTM-1, CNTM-2 and CNTM-3.

The reference material, a physical mixture of NTM composite and carbon black, was prepared as well, of which carbon amount was set as 1.5. The reference material was named as C&NTM.

3.2.2 Characterization

X-ray diffraction (XRD) patterns were recorded by using Cu Kα radiation (λ = 1.5418

Å) on a Rigaku Rint2100 operation at 40 kV and 30 mA with 0.25° divergence slit, 0.5° antiscatter slit, between 1 and 60° (2θ). The crystallite sizes of TiO_2 particles were calculated by Scherrer's equation for the (*101*) reflection at about 2θ = 25°. UV-vis diffuse reflectance spectra were measured at room temperature in air on a Shimadzu UV-2450 photometer over the range 200 to 800 nm, while $BaSO_4$ was used as a reference. Chemical contents of each sample was analyzed by energy dispersive spectra (EDS, JED-2300) measurements which was equipped on scanning electron microscopy (SEM, JSM-6380A). Surface analysis based upon the N_2 adsorption/desorption technique was conducted on a BELSOP18SP automated gas adsorption analyzer at 77 K after sample pretreatment at 110°C for 12 h under vacuum. S_{BET} values were calculated by the Brunauer-Emmet-Teller (BET) method*[18]* from the linear part of BET plot according to IUPAC recommendations*[19]* using the adsorption isotherm (relative pressure (P/P_0) = (0.08-0.30). Pore size distributions were calculated from the adsorption isotherms by the Barrett-Joyner-Halenda (BJH) method*[20]* and the total pore volume was obtained from the maximum adsorption at P/P_0 of 0.999. Thermogravimetric and differential thermal analysis (TG-DTA) curves were recorded on a TG8120/SH instrument from room temperature to 1000°C at a heating rate of 10°C min^{-1} under air using R-Al_2O_3 as the standard material. Photoluminescence (PL) spectra were measured at room temperature with a Hitachi F-2500 fluorospectrophotometer using 420 nm Ar^+ lasers as excitation sources.

3.2.3 Evaluation of photocatalytic activity

The photocatalytic activity of NTM was evaluated by photodecomposition of BPA in aqueous solution. A catalyst loading of 100 mg per 100 mL of solution was used. The initial concentration of BPA was 10 ppm. The suspension contained in a Pyrex glass beaker was placed in a thermostatic water bath at constant 25°C for 1 h of magnetic stirring in the dark to reach to the adsorption–desorption equilibrium of BPA. Subsequently, the photodecomposition of BPA was performed under visible light

irradiation by using a Xe lamp(BA-X502) equipped with both UV filter and IR filter to select the required wavelength (420 nm < λ < 1200 nm). The intensity of the light source was fixed at 10 mW/cm^2 and the vertical distance from the lamp to the surface of suspension was also fixed at about 20 cm. The concentration of BPA was analyzed by using HPLC(Shimadzu LC-20AT) instrument equipped with a UV-vis detector and a C18 separation column (5 μm, 150 × 4.6 mm). The elution was monitored at 254 nm. The mobile phase was a mixture of acetonitrile and water (50 / 50, v / v), which was pumped at a flow rate of 1.0 mL min^{-1}.

Table 3.1 Conditions of photodecomposition

Concentration of BPA	10 ppm
Solution volume	200 mL
Temperature	25°C
Catalyst dosage	0.1 g（1.0 g/L）
Light source	300 W Xe lamp
Irradiation intensity	10 mW/cm^2（420 nm < λ < 1100 nm）

3.3 Results and discussion

3.3.1 Characterization

The XRD patterns of NTM, CNTM-1.0 and C&NTM sample are shown in Fig. 3.2. The CNTM-1.0 and the C&NTM sample exhibit very similar patterns to the NTM sample, indicating that the basic structure of CNTM-1.0 sample was not changed by introducing carbonaceous species. The TiO_2 phase in all the samples were identified as only anatase(as shown at 2θ = 25.3°, 37.9°, 47.6°, 54.8°). In the case of CNTM-1.0 and C&NTM sample, no carbon phase was characterized. It is suggested that carbonaceous species the introduced into CNTM-1.0 composite are supposed to be amorphous carbon. Fig. 3.3 shows the XRD patterns of CNTM-1.0 composite added with different ethanol dosage from 0.5 to 2. The similar patterns indicated the same crystalline structure.

The UV-vis diffuse reflection spectra of the NTM, CNTM-1.0 and C&NTM samples are shown in Fig. 3.4. The color of NTM sample exhibited light ivory color. In contrast, the CNTM-1.0 and C&NTM samples show obviously strong absorbance in the visible light region due to the introduced carbon. Whereas the CNTM-1.0 sample exhibit lower absorbance compared with C&NTM sample even though the carbon content of two samples was almost same. This result revealed that the deposited carbonaceous species in CNTM-1.0 sample is not similar to carbon black. Fig. 3.5 shows the UV-vis spectra of CNTM composite added with different ethanol dosage from 0.5 to 2. It is easy to find out that the absorbance of the samples is enhanced in sequence following with the carbon content (as shown in Table 3.2) of the samples with increasing ethanol dosage from 0.5 to 2.0 mL.

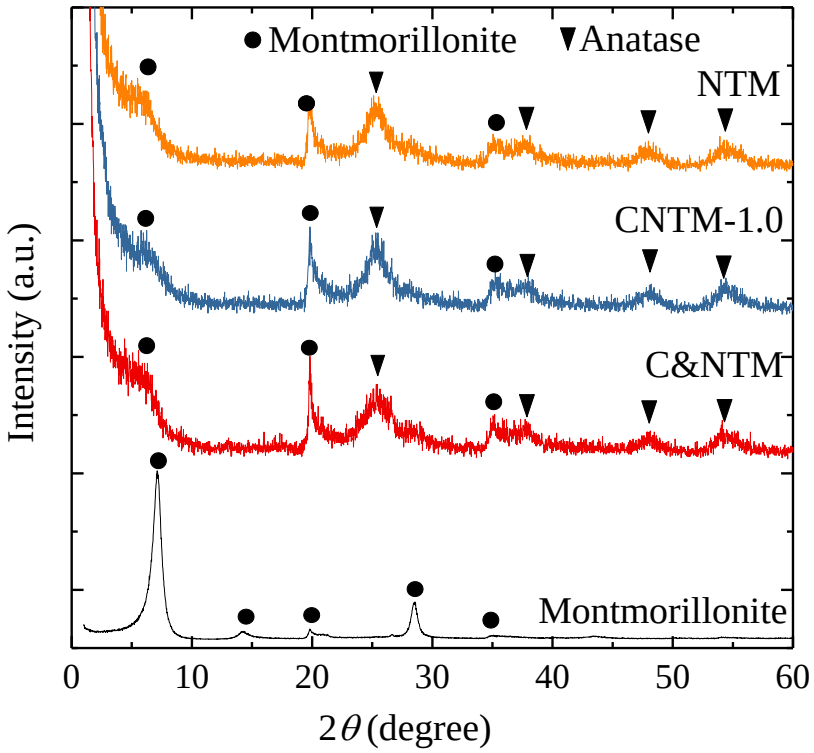

Fig. 3.2 XRD patterns of NTM, CNTM-1.0 and C&NTM sample.

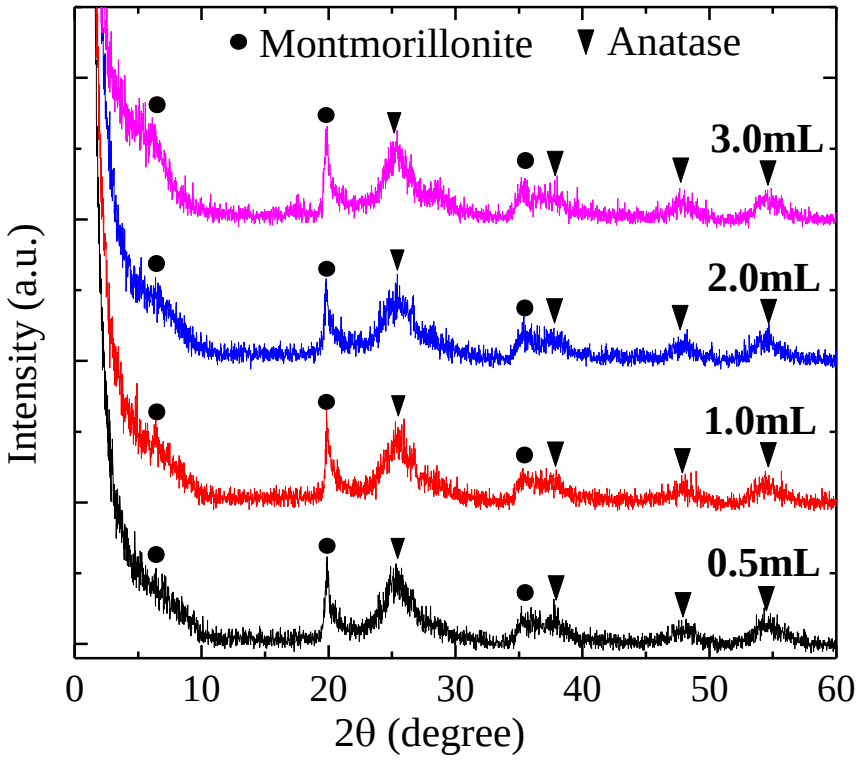

Fig. 3.3 XRD patterns of CNTM composite added with different ethanol dosage from 0.5 to 2.

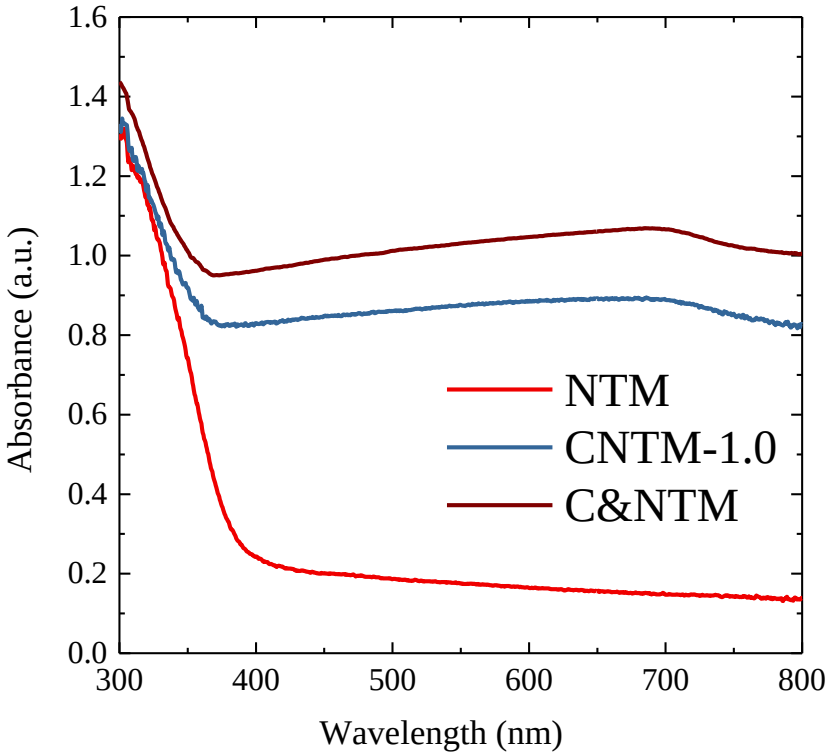

Fig. 3.4 UV-vis spectra of NTM, CNTM-1.0 and C&NTM sample.

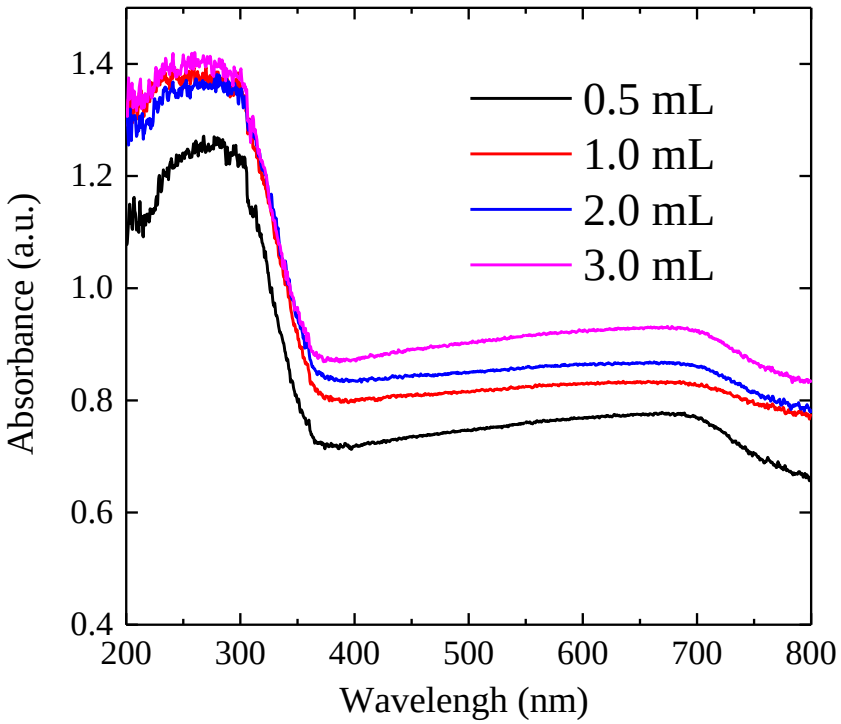

Fig. 3.5 UV-vis spectra of CNTM composite added with different ethanol dosage from 0.5 to 2.

Table 3.2 The chemical content of various samples (mass %)

Sample	NTM	C&NTM	CNTM-0.5	CNTM-1	CNTM-2	CNTM-3
C	-	1.0	0.9	1.1	1.5	1.8
N	6.0		6.5			
TiO_2	32.2		28.5			
SiO_2	43.5		45.6			
Al_2O_3	15.6		15.7			
MgO	2.4		2.3			
Fe_2O_3	1.1		1.1			

The N_2 adsorption and desorption isotherms of CNTM-1.0 and NTM samples are shown in Fig. 3.6a. The isotherm curves show a steeply increased adsorption at low P/P_0 values and hysteresis loop at intermediate P / P_0 values, which are similar to the characteristic type IV, indicating the existence of micropores and mesopores*[21]*. The shape of the hysteresis loops is similar to type H3, reflecting the slit shaped pores resulted from the layered structure stacked by montmorillonite sheets*[22,23]*. The pore size distributions of CNTM-1.0 and NTM composites are calculated from the N_2 isotherms and are shown in Fig. 3.6b. The majority of the pores in CNTM-1.0 and NTM samples are micropores (< 2 nm) arose from the intercalation of TiO_2 particles into the interlayer space of montmorillonite. As shown in Table 3.3, the NTM sample exhibits 193 m^2/g of specific surface area, 0.28 cm^3/g of pore volume and 5.3 nm of pore size while the CNTM-1.0 sample exhibits slightly increased specific surface area (215 m^2/g) and very similar pore volume (0.25 cm^3/g) and pore size (5.2 nm). This result probably suggested that the carbonaceous species arisen by carbon deposition didn't change the surface structure of the NTM composite.

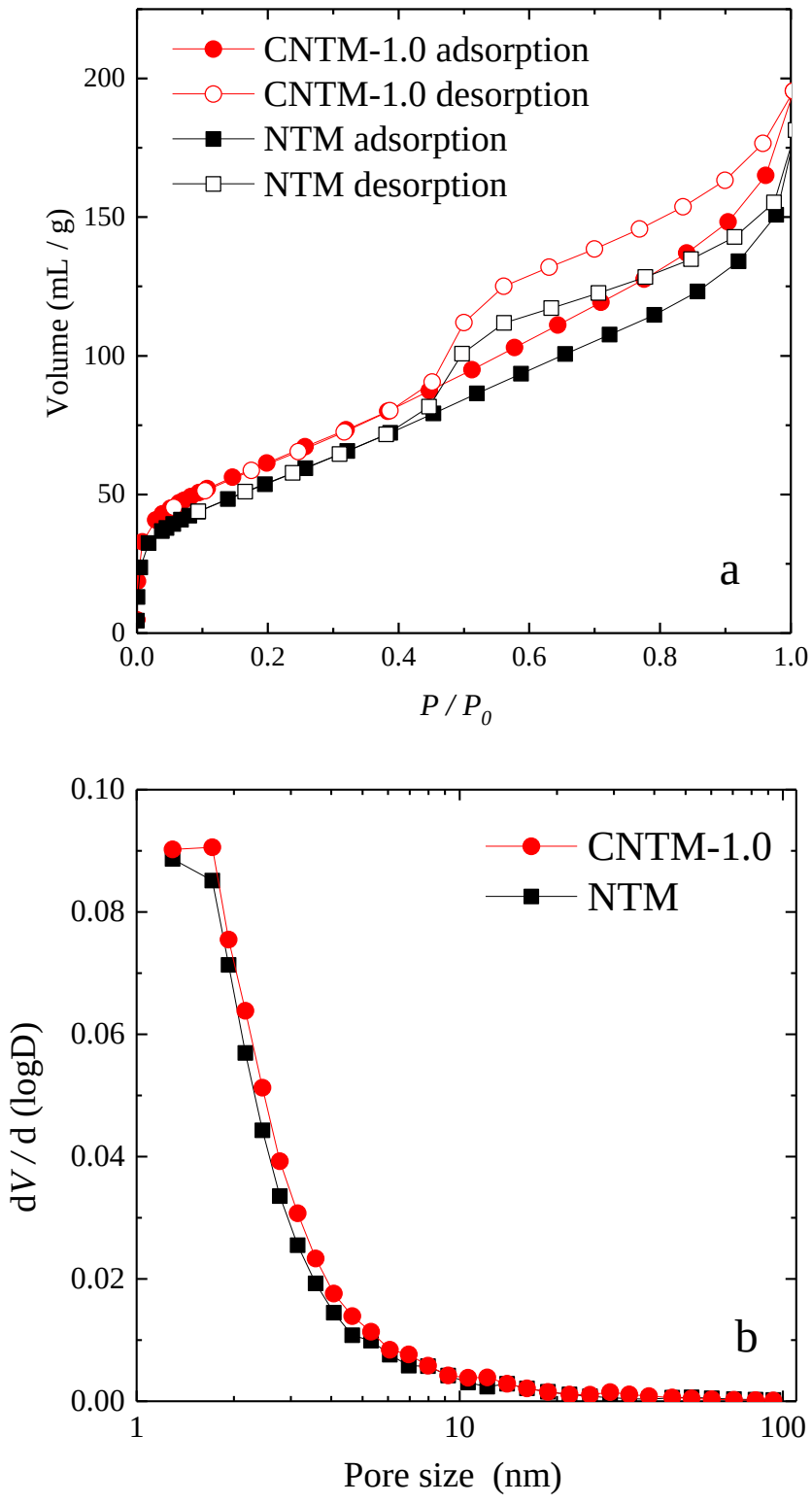

Fig. 3.6 N_2 adsorption isotherms of NTM and CNTM-1.0 samples.

Table 3.3 Specific surface area, pore volume and average pore size.

Sample	S_{BET} [m^2/g]	Vt [cm^3/g]	d [nm]
CNTM-1.0	215	0.25	5.2
NTM	193	0.28	5.3

The TG/DTA curves of the CNTM-1.0 and NTM samples are shown in Fig. 3.7. The TG curves of the both samples show a rapid weight loss below 150°C. With the temperature increasing, CNTM-1.0 sample exhibits much faster weight loss than NTM from 200 °C to 500 °C. The subsequent fast weight loss was appeared from 550 °C to 700 °C. The endothermic peaks were detected at 103 °C for CNTM-1.0 sample and 98 °C for NTM sample, respectively, indicating the evaporation of water*[24]* physisorbed on the surface of the samples. The lower intensity of the endothermic peak of CNTM-1.0 sample revealed the lower water adsorption due to the fact that the introduced carbonaceous species may change the surface hydrophilic/hydrophobic property. The thermic curve of CNTM-1.0 sample exhibits a broad exothermic peak over the range of 200 °C to 500 °C, which may indicate the oxidation process of carbonaceous species*[25]*. The subsequent endothermic peaks were observed at 633 °C (CNTM-1.0) and 634 °C (NTM), respectively, associated with the dehydroxylation of the silicate layers of montmorillonite*[26,27]*.

PL spectra have been widely used to understand the fate of electron−hole pairs in semiconductors*[28-30]*. Due to the fact that the recombination of photoexcited electrons and positive holes result in PL emission, the lower PL intensity indicates a lower recombination rate. In order to investigate the photocatalytic activity, PL spectra was recorded as shown in Fig. 3.8. The PL spectra display a broad emission peak around 520 nm under bandgap excitation, arising from oxygen vacancies and defects on the surface of TiO_2 particles*[31,32]*. According to the results, the PL intensity of NTM sample is quite high, whereas that of both the CNTM-1.0 and the C&NTM samples are rather low. Compared with the C&NTM sample, the CNTM-1.0 sample exhibits much lowered PL intensity. Although both kinds of carbon (dispersed carbon black in C&NTM and deposited carbon in CNTM-1.0) may possibly absorb part of the fluorescence generated from TiO_2 at the moment PL phenomenon occurred, the much

lowered PL intensity of CNTM-1.0 sample revealed that the recombination of photoexcited electrons and positive holes in CNTM-1.0 sample was greatly restrained.

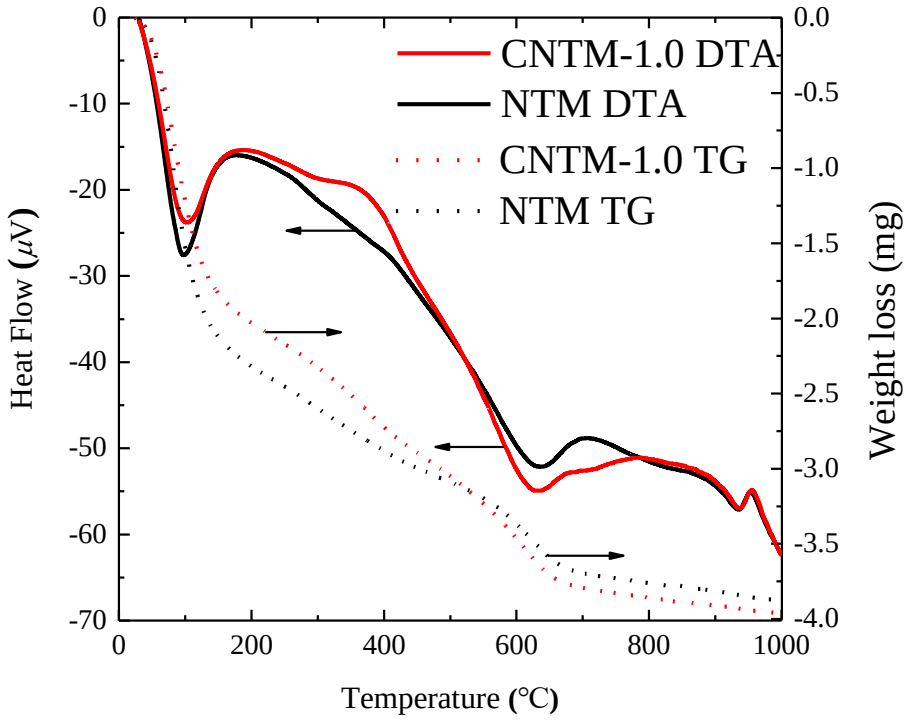

Fig. 3.7 TG/DTA curves of the CNTM-1.0 and NTM samples.

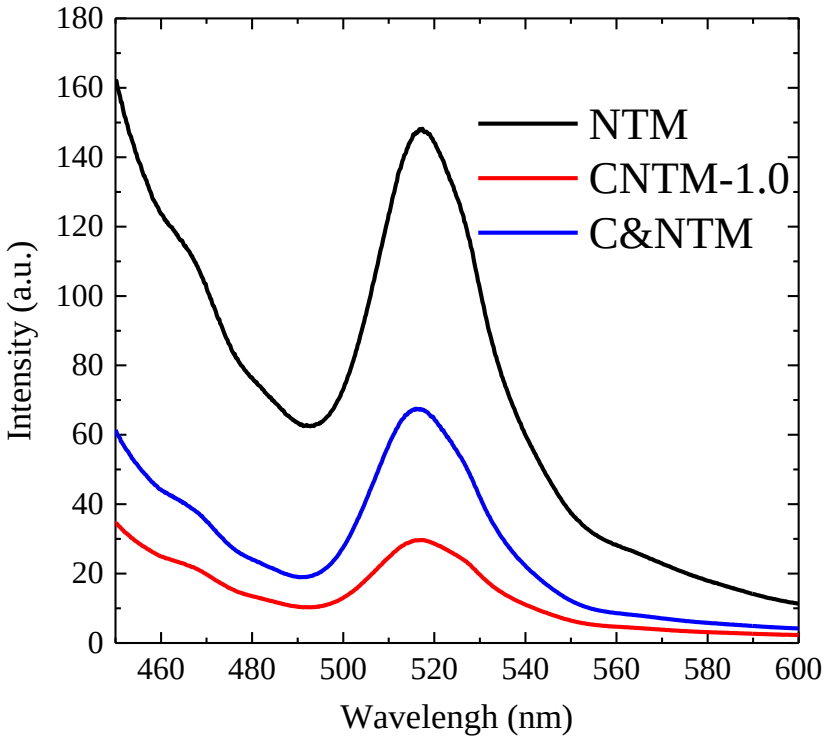

Fig. 3.8 PL spectra of NTM, CNTM-1.0 and C&NTM sample.

3.3.2 Photocatalytic activity of carbon deposited N-doped TiO_2/montmorillonite.

The photocatalytic activities of CNTM-1.0 samples and that of reference materials were evaluated by decomposition of BPA and the results are shown in Fig. 3.9. The curves show that the photocatalytic activity of the CNTM-1.0 sample was the highest. The C&NTM sample exhibits obvious adsorption to BPA after keeping in the dark for 1 hour, whereas in the case of NT, NTM and CNTM-1.0 samples, the adsorption to BPA was very low and almost negligible. According to these results, it should be noted that the introduced carbon in C&NTM and CNTM-1.0 samples are quite different. For C&NTM sample, the introduction of carbon black seems to greatly suppress the photocatalytic activity although the adsorption property was increased. In the case of CNTM-1.0 sample, the deposited carbonaceous species by carbon modification have greatly increased the photocatalytic activity in spite of negligible effect on adsorption behavior. The decomposition rates (per mass. TiO_2) of BPA by CNTM-1.0 composite and that of reference materials were calculated and the results are shown in Fig. 3.10. The CNTM-1.0 sample exhibits much higher decomposition rate than that of NTM sample, indicating that the recombination of photoexcited electrons and positive holes are probably restrained by the deposited carbonaceous species in CNTM-1.0 composite. In the case of C&NTM sample, the decreased photocatalytic activity should be attributed to the fact that the carbon black were not immobilized on the surface of NTM composite. During the photocatalysis process, most carbon black particles float on the top of the BPA aqueous solution, and thus blocked the vertical irradiation light reaching to the TiO_2 particles, leading to inadequate photocatalysis reaction.

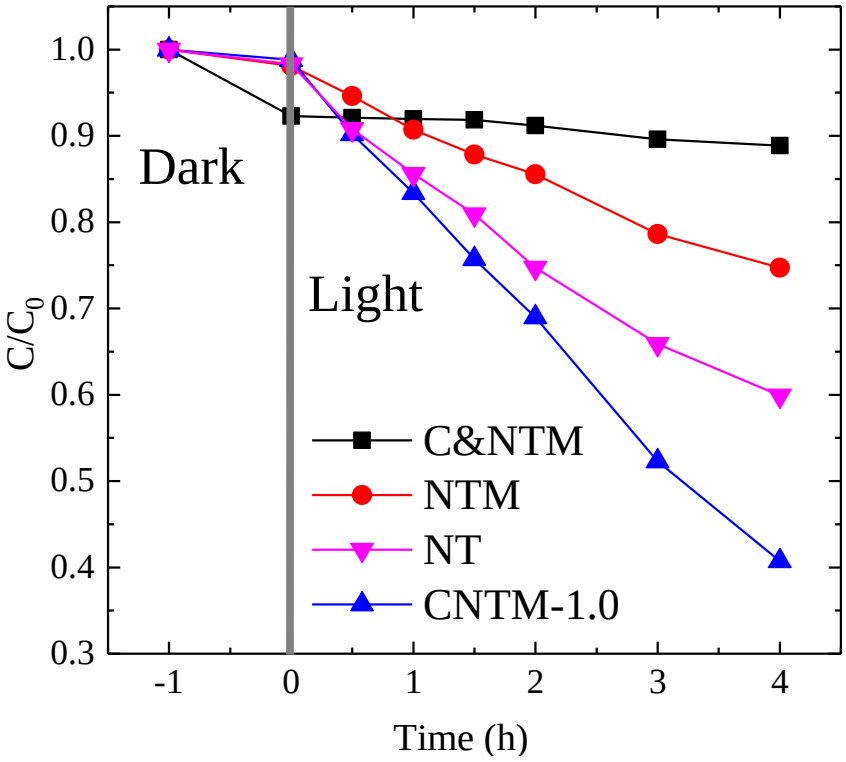

Fig. 3.9 Decomposition curves of BPA by C&NTM, NTM, NT and CNTM-1.0 samples.

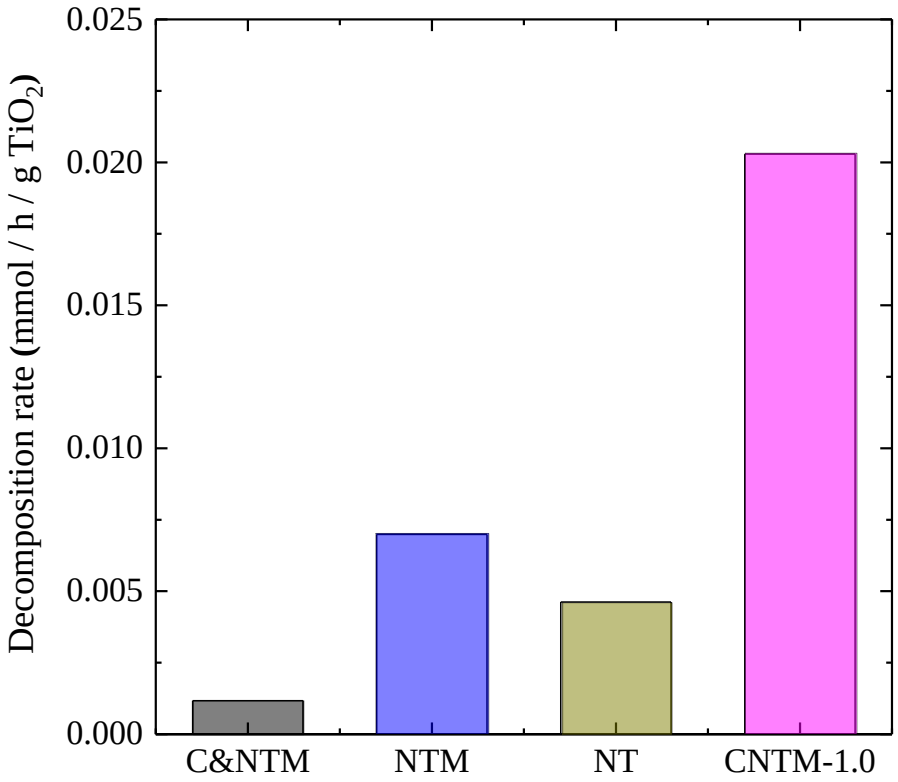

Fig. 3.10 Decomposition rates of by BPA C&NTM, NTM, NT and CNTM-1.0 samples.

3.3.3 Effect of carbon content on photocatalytic activity

The photocatalytic activities of CNTM composites with different ethanol dosages were evaluated by decomposition of BPA and the results are shown in Fig. 3.11. The CNTM composite with the ethanol dosage of 2 mL/g composite shows the highest photocatalytic activity. It should be noted that the dark adsorption behaviors of all the four samples were almost similar and in each case a very low adsorption was observed. Thereby, the role of adsorption is almost negligible while considering the photocatalytic decomposition of BPA becomes more important.

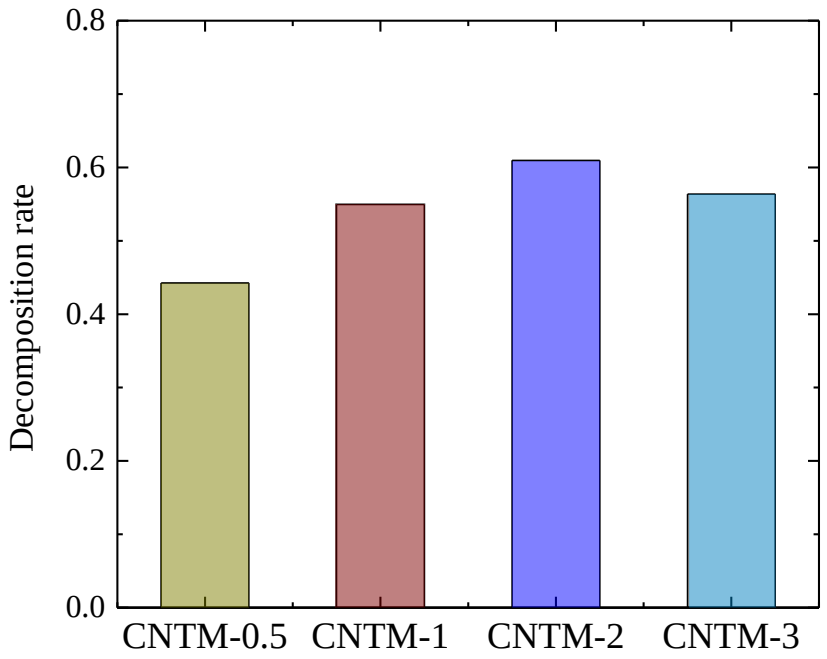

Fig. 3.11 Decomposition curves of CNTM composites with different ethanol dosage.

3.4 Conclusion

Carbon deposited N-doped TiO_2/montmorillonite composite was prepared with carbon modification with adding ethanol into dried N-doped TiO_2/montmorillonite colloidal，treating with calcination. Carbonaceous species were generated at the nano size and deposited in the interlayer space. These nano-sized carbonaceous species resulted in remarkable enhancement of photocatalytic activity on decomposition of BPA under visible light irradiation and negligible effect on adsorption of BPA. The improved photocatalytic activity was due to the fact that the recombination of photoexcited electrons and positive holes is restrained by the deposited carbonaceous species, leading to long-lived positive holes that play a very important role in photocatalysis. Furthermore, the effect of carbon content on photocatalytic activity was discussed. The results show that the carbon content depended on ethanol dosage and the optimum ethanol dosage was 2 mL/g. Heavy ethanol dosage resulted in excessive carbonaceous species which may cause interference from absorbing visible light.

3.5 Reference

1. Y. Yamada, Y. Kanemitsu, Determination of electron and hole lifetimes of rutile and anatase TiO2single crystals. Appl. Phys. Lett. 101 (2012) 133907.
2. M. V. Dozzi, C. D' Andrea, B. Ohtani, G. Valentini, E. Selli, Fluorine-Doped TiO2 Materials: Photocatalytic Activity vs Time-Resolved Photoluminescence J. Phys. Chem. C 117 (2013) 25586–25595.
3. S. Sato, R. Nakamura, S. Abe, Visible-light sensitization of TiO_2 photocatalysts by wet-method N doping, Appl. Catal. A: Gen. 284 (2005) 131–137.
4. S. Sakthivel, H. Kisch, Photocatalytic and Photoelectrochemical Properties of Nitrogen-Doped Titanium Dioxide, Chem. Phys. Chem. 4 (2003) 487–490.
5. H. Kisch, S. Sakthievel, M. Janczarek, D. Mitoraj, A low-band gap, nitrogen-modified titania visible-light photocatalyst, J. Phys. Chem. C. 109 (2007) 11445–11449.
6. G. Barolo, S. Livraghi, M. Chiesa, M. C. Paganini, and E. Giamello, Mechanism of the photoactivity under visible light of N-doped titanium dioxide. Charge carriers migration in irradiated N-TiO_2 investigated by electron paramagnetic resonance. J. Phys. Chem. C. 116 (2012) 20887–20894.
7. H. Irie, Y. Watanabe, and K. Hashimoto, Nitrogen-concentration dependence on photocatalytic Activity of $TiO_{2-x}N_x$ powders, J. Phys. Chem. B. 107 (2003) 5483-5486.
8. S. Yamanaka, T. Nishihara and M. Hattori, Preparation and properties of titania pillared clay, Mater. Chem. Phys. 17 (1987) 87–101.
9. J. Sterte, Synthesis and properties of titanium oxide cross-linked montmorillonite, clays Clay Mineral. 34 (1986) 658–664.
10. C. Ooka, H. Yoshida, K. Suzuki, T. Hattori, Highly hydrophobic TiO2 pillared clay for photocatalytic degradation of organic compounds in water, Micropor. Mesopor. Mater. 67 (2004) 143–150.
11. Y. Kameshima, Y. Tamura, A. Nakajima, K. Okada, Preparation and properties of TiO2/montmorillonite composites, Applied Clay Science. 45 (2009) 20–23.
12. T. Matsunaga, M. Inagaki. Carbon-coated anatase for oxidation of methylene blue and NO. Appl. Catal. B. 64 (2006) 9–12.
13. M. Inagaki, F. Kojin, B. Tryba, M. Toyoda. Carbon-coated anatase: the role of the carbon layer for photocatalytic performance. Carbon. 43 (2005) 1652–1659.
14. C. C. Mao, H. S. Weng. Promoting effect of adding carbon black to TiO_2 for aqueous photocatalytic degradation of methyl orange. Chem. Eng. J. 155 (2009) 744–749.
15. C. Lettmann, K. Hildenbrand, H. Kisch, W. Macyk, WF. Maier. Visible light photodegradation of 4-chlorophenol with a coke-containing titanium dioxide photocatalyst. Appl. Catal. B. 32 (2001) 215–227.
16. S. Sakthivel, H. Kisch. Daylight photocatalysis by carbon modified titanium dioxide. Angew Chem. Int. Ed. 42 (2003) 4908–4911.
17. J. Zhong, F. Chen, J. Zhang. Carbon-deposited TiO_2: synthesis, characterization,

and visible photocatalytic performance. J. Phys. Chem. C. 114 (2010) 933–939.
18. S. Brunauer, P.H. Emmet, E. Teller, Adsorption of gases in multimolecular layers. J. Am. Chem. Soc. 60 (1938) 309-319.
19. K.S.W. Sing, D.H. Everett, R.A.W. Haul, L. Moscou, R.A. Pierotti, J. Rouquerol, T. Siemieniewska, Reporting physisorption data for gas/solid systems with special reference to the determination of surface area and porosity, Pure Appl. Chem. 57 (1985) 603–619.
20. E.P. Barrett, L.G. Joyner, P.P. Halenda, The determination of pore volume and area distributions in porous substances. I. Computations from nitrogen isotherms. J. Am. Chem. Soc. 73 (1951) 373–380.
21. F. Rouquerol, J. Rouquerol, K. Sing, Adsorption by Powders and Porous Solids: Principles, Methodology and Applications. Academic Press, London (1999).
22. Y. Kameshima, T. Koike, T. Isobe, A. Nakajima, K. Okada. Effect of the SiO_2/TiO_2 ratio on the solid acidity of SiO_2–TiO_2/montmorillonite composites. Materials Research Bulletin. 44 (2009) 1906–1909.
23. Y. Kameshima, A. Yoshizawa, A. Nakajima, K. Okada. Solid acidities of SiO2 – TiO2/montmorillonite composites synthesized under different pH conditions. Applied Clay Science. 46 (2009) 181–184.
24. T. Mishra, K. Parida. Transition metal pillared clay 4. A comparative study of textural, acidic and catalytic properties of chromia pillared montmorillonite and acid activated montmorillonite. Applied Catalysis A: General. 166 (1998) 123-133.
25. J. Zhong, F. Chen, J. Zhang. Carbon-Deposited TiO_2: Synthesis, Characterization, and Visible Photocatalytic Performance. J. Phys. Chem. C. 114 (2010) 933–939.
26. K. Mogyorósi, I. Dékány, and J. H. Fendler. Preparation and Characterization of Clay Mineral Intercalated Titanium Dioxide Nanoparticles. Langmuir. 19(2003)2938–2946
27. D. Chen, G. Du, Q. Zhu, F. Zhou. Synthesis and characterization of TiO2 pillared montmorillonites: Application for methylene blue degradation. Journal of Colloid and Interface Science. 409 (2013) 151–157.
28. J.G. Yu, H.G. Yu, B. Cheng, X.J. Zhao, J.C. Yu, W.K. Ho. The effect of calcination temperature on the surface microstructure and photocatalytic activity of TiO_2 thin films prepared by liquid phase deposition. J. Phys. Chem. B. 107 (2003) 13871–13879.
29. Cong, Y.; Zhang, J.; Chen, F.; Anpo, M. Synthesis and characterization of nitrogen-doped TiO_2 nanophotocatalyst with high visible light activity. J. Phys. Chem. C. 111(2007) 6976−6982.
30. T. Tsubota, A. Ono, N. Murakami, T. Ohno. Characterization and photocatalytic performance of carbon nanotube material-modified TiO_2 synthesized by using the hot CVD process Applied Catalysis B: Environmental. 91 (2009) 533–538
31. W. Tu, Y. Zhou, Q. Liu, S. Yan, S. Bao, X. Wang, M. Xiao, Z. Zou. An in situ simultaneous reduction-hydrolysis technique for fabrication of TiO_2 -graphene 2d

sandwich-like hybrid nanosheets: graphene-promoted selectivity of photocatalytic-driven hydrogenation and coupling of CO_2 into methane and ethane. Adv. Funct. Mater. 23 (2013) 1743–1749.

32. W. Qian, P. A. Greaney, S. Fowler, S. Chiu, A. M. Goforth, J. Jiao. Low-temperature nitrogen doping in ammonia solution for production of N-doped TiO_2-hybridized graphene as a highly efficient photocatalyst for water treatment, ACS Sustainable Chem. Eng. 2 (2014) 1802−1810.

Chapter 4 Conclusion

In this thesis, in order to develop an effective and environment-friendly water treatment method for decomposition of hazardous organic materials in wastewater, high performance TiO_2/clay composite was prepared. Two modification methods, nitrogen doping and carbon deposition were both employed to improve the photocatalytic activity of TiO_2/clay composite. The visible light response was enhanced to TiO_2/clay composite by nitrogen doping. Meanwhile, the photocatalytic activity was further improved under visible light irradiation due to carbon deposition. This thesis is constructed with four chapters and summarized below:

In Chapter 1, the background of water pollution and the overview of TiO_2 catalyst and TiO_2/clay composite were introduced. Meanwhile, the object of this thesis, to develop high active visible light responsive TiO_2/clay composite, has been proposed, accordingly.

In Chapter 2, the nitrogen doped TiO_2/montmorillonite composite was prepared via a sol-gel method, in which urea is introduced into TiO_2 sol. Two points, the effect of the N / Ti ratio on photocatalytic activity and the effect of calcination temperature on photocatalytic activity were mainly discussed, via characterization and evaluation of photocatalytic activity. According to the characterization results, the phase of the intercalated TiO_2 particles in all samples was identified as anatase. The absorbance around 400 to 600 nm enhanced gradually by increasing the N / Ti ratio of the NTM composite. When raise the calcination temperature, the absorbance enhanced gradually, but stop to decrease over 350°C. The decreased absorbance was attributed to the fact that calcination leads to nitrogen loss at high temperature. The decomposition of BPA was carried out for evaluation of photocatalytic activity. According to the results, it is worth to notice, that the decomposition of BPA in the dark or without a photocatalyst was almost negligible. Consequently, the adsorption behavior of BPA is almost negligible and discussion on photodecomposition of BPA becomes much more important. When the N / Ti ratio of the NTM composite was increased, the decomposition rate of BPA increased with the N/Ti ratio up to 1.5, and then started to decrease gradually. The optimum calcination temperature was 250°C. With further raising the calcination temperature, the photocatalytic activity decreased. This result is

not quite in accordance with that of other reports, however, it was in excellent agreement with the reference nitrogen doped TiO_2 which is prepared with the same method but without montmorillonite.

In Chapter 3, the carbon deposited N-doped TiO_2/montmorillonite composite was prepared with carbon modification. Ethanol, as a carbon source, was added into the N-doped TiO_2/montmorillonite colloidal, treating with low temperature calcination. Characterization and evaluation were carried out in order to understand the differences between the NTM composite and CNTM composite and the effect of carbon content on photocatalytic activity. According to the characterization results, the carbon modification has made a great effect on the properties of the CNTM composite. An obviously color change over the visible light region was attributed to carbon modification. The absorbance of the CNTM composite depended on carbon content which increased with increasing ethanol dosage. Due to no observable carbon phase was observed, the carbonaceous species introduced into the CNTM composite are supposed to be amorphous carbon. These carbonaceous species were generated at nano size and deposited in the interlayer space, resulting increase of specific surface area and decrease of both average pore size and average pore volume. In the case of photocatalytic activities, it is worth to notice that the carbon modification resulted in remarkable enhancement of photocatalytic activity on decomposition of BPA under visible light irradiation and negligible effect on the adsorption behavior of BPA. The high photocatalytic activity of the CNTM composite was due to the synergy effect of nitrogen doping and carbon deposition. Firstly, nitrogen doping enabled visible light response of TiO_2 particles in the composite, leading to photoexcitation of electrons and positive holes under visible light irradiation. Meanwhile the carbonaceous species act as charge accepter so that electrons or holes can transfer from TiO_2 particles to carbonaceous species freely, thus retarded the recombination of photoexcited electrons and positive holes. Consequently, the longtime lived electrons and positive holes had increased chance to react with the adsorbates in photocatalysis reaction. Furthermore, the effect of carbon content on photocatalytic activity was discussed. The results show that the carbon content depended on ethanol dosage and make an obvious effect on photocatalytic activity. The optimum ethanol dosage was 2 mL/g. Heavy ethanol dosage resulted in an excessive amount of carbonaceous species, which may cause interference to TiO_2 particles from absorbing visible light.

In Chapter 4, the summary of this thesis was provided and the prospects of this research were placed.

In view of the results above, this thesis is expected to be valuable for the researches on improvement of the photocatalytic activity of TiO_2 catalyst. In addition, it is hoped that this research will contribute to the development of environment-friendly water treatment and be helpful to restrain water pollution.

Acknowledgements

At first, I would like to show deepest appreciation and gratitude to Prof. Yoshikazu Kameshima, my supervisor. His guidance, sincerity, generosity and patience greatly helped me to complete this thesis. His guidance enlightens me not only in this thesis but also in my future study. I would also like to show deep gratitude to Prof. Michihiro Miyake, my co-supervisors, who gave me the opportunity to study in this lab. I would like to express my heartfelt gratitude to Prof. Shunsuke Nishimoto. His advice and instruction also helped a lot on my study.

Secondly, I would like to show gratitude to Prof. Nanba and Prof. Benino for their guidance and support on using equipment. Without their help, this thesis wouldn't successfully completed.

At last, I am very thankful to all the students in both of Miyake lab and Kameshima lab for their friendly behavior, their great cooperation during my study life in Japan.